Atmospheric Spray Freeze-Drying on Common Biologics and Excipients as a Comparison to Lyophilization

by

Alvin Ly

A thesis submitted in partial fulfillment of the requirements for the degree of

Master of Science

Department of Mechanical Engineering

University of Alberta

Abstract

Atmospheric spray freeze-drying (ASFD) is an alternative freeze-drying process to conventional vacuum freeze-drying. ASFD involves spray-freezing biologics of interest in a feedstock into a cold freezing chamber. Cold drying gas passes through the chamber at a high flow rate to sublime the water and ice in the powder with convective forces. ASFD is a seven-hour drying process compared to conventional freeze-drying which is in the order of days. Ertapenem, a regularly used antibiotic, and trehalose, a biologic stabilizer in freeze-drying, were freeze-dried at varying feedstock concentrations. Ertapenem was freeze-dried at 50, 100, 150, and 200 mg/mL; higher concentrations had pale yellow discoloration in both liquid and dried powder. Although ASFD ertapenem was porous compared to the lyophilized counterpart, higher feedstock concentrations yielded larger particles with lower porosity. Trehalose was freeze-dried at 100, 200, and 300 mg/mL. ASFD trehalose at lower concentration existed as a free-flowing powder whereas higher feedstock concentration yielded a thin brittle cake. Both trehalose and ertapenem powders at lower feedstock concentrations made powders with large pores and high void fraction, which is predicted to have excellent wetting and aerodynamic properties. Bacteriophage D29 in solutions with varying concentration of mannitol and trehalose, were freeze-dried using ASFD. A solution of trehalose and mannitol at a mass ratio of 7:3 and a total feedstock concentration of 100 mg/mL had the lowest titer reduction of ~0.6 logs with a powder moisture content of 4.9±0.1 %. In comparison, pure trehalose and 1:1 ratio of trehalose and mannitol both had titer reductions larger than 1.5 logs. Raman spectroscopy of the powders showed that trehalose in the powder remained amorphous while mannitol completely crystallized, which are desirable for preserving phages in a dry solid form. The short drying process, improved wetting properties, and the ability to preserve bacteriophages makes ASFD an attractive alternative to conventional freeze-drying.

Preface

This thesis manuscript contains work that has been co-authored and submitted for publication as well as some unpublished work. I am the primary author of Chapter 3 of this thesis, which has been submitted to a peer-reviewed journal that is currently under review. The co-authors to that chapter include Nicholas B. Carrigy, Hui Wang, Melissa Harrison, Dr. Dominic Sauvageau, Dr. Andrew R. Martin, Dr. Reinhard Vehring, and Dr. Warren H. Finlay. Hui Wang performed Raman spectroscopy analysis and assisted in writing the Raman spectroscopy sections of Chapter 3. The titer measurements for evaluating the phage activity of phage D29 was performed by Melissa Harrison. The atmospheric spray freeze-drying (ASFD) apparatus was originally built by Zhaolin Wang. I modified the ASFD apparatus and performed all the experiments presented in the thesis. The lyophilized ertapenem was provided to our lab by Pfizer Canada as part of a research partnership through the Mitacs program funded by Natural Sciences and Engineering Research Council of Canada (NSERC). I drafted all the sections of this thesis with significant editorial contributions and expert opinion from Dr. Warren H. Finlay and all the co-authors involved in Chapter 3.

Acknowledgement

I would like to dedicate this section to thank my friends, family, and colleagues that have supported me throughout this chapter in my life. I am blessed with a great support system that have helped me through the lows and celebrated with me through the highs.

I am privileged and lucky to work under such a great supervisor, Dr. Warren Finlay. I appreciate all the help and mentorship you have given me throughout this project. As my supervisor, you have given me the freedom to manage my project with my own style, make mistakes and grow from them. On the same note, you have always been there to guide me through my project, from the quick meetings in your office, where I can come in a moment's notice, to the frequent lab visits in ensuring success in my research project. Thank you for the opportunity to study under you and to work in an amazing environment.

I would also like to thank Dr. Andrew Martin for being an amazing co-supervisor. Your positive attitude as an instructor for "Mechanics of Respiratory Drug Delivery" engaged me as a student and encouraged me to learn more about the field. Whenever I get overwhelmed with experiment results or analysis, you would show up at the lab and help me take a step back and simplify the necessary steps and realize how much I have already completed. It is always easy to talk to you about the stresses of graduate studies since you have also studied here at the University of Alberta and can always relate and advise me. Thank you for all the support and ideas you have given me throughout my research.

I would like to thank Dr. Vehring for his support and guidance throughout my studies. His extensive knowledge on powder formation, solid phase properties, and bacteriophages have guided me in submitting a paper for publication. Dr. Vehring's interest in my study did not stop at just the experiments and results but also a vision of how impactful these studies are to society; these insights have helped me acknowledge the importance of the work our lab does. I would also like to thank Luba Slabyj for her help in editing and proofreading my work.

I am lucky to have great colleagues and labmates to work with throughout my project. I am grateful to have Helena Orszanska in our lab in helping me with lab work, research, and experiments. I am thankful for your help in formulation preparation, powder sample analysis, and experiment advice. Your enthusiasm in my research project are contagious and our discussions

about bacteriophage, formulation, and antibiotic encourage me in generating new ideas. I appreciate your patience in teaching a mechanical engineering student about protein denaturation and hydrolysis. By providing me with insightful feedbacks after every experiment and relative research articles, my background knowledge about freeze-drying has improved drastically and have been crucial in the completion of my project. I would also like to thank everyone in my lab for the continuous help and support. Scott Tavernini, you helped me more than you know, it helps bouncing ideas off you, ranting about failed experiments, and just chatting about things going on in our lives. Connor Ruzycki, I see you as the big brother of our lab, it is always nice knowing someone with so much research experience is in our lab that can always give impactful feedback. Milad Kiaee, I enjoyed all our conversations that range from politics to video games. Nick Carrigy and Hui Wang, although we are in different buildings you guys have been instrumental to my work in bacteriophages and Raman spectroscopy and never hesitated to help me, thank you guys so much! I would also like to thank John, Tyler, Paul and Kineshta, our occasional lab get together are always so fun.

My family has been one of the best support systems I have. Mom and dad, you have always believed in me and never doubted if I could accomplish my goals. You have instilled values of integrity, hard work, and happiness in me. I am now legally obligated to work with ethics and morals in mind but I believe you have taught me all of these things well before I first stepped into the university. I am thankful for all you have done and all you have sacrificed for me. Newson, my brother, you have always watched over me since I was a kid and I hope you are proud of how much I have grown. Sevea, my sister, I have never told you how much I appreciate our chats, our hangouts and our fights. It is relieving knowing that you will always have my back, no matter where life takes me. I would like to thank all my friends, the ones that have become like family, and to the ones I have met throughout this time.

I am thankful to work with Pfizer on my project. I would like to thank Antoine Cournoyer for his interest in the research project and the continual guidance and support throughout my degree. I would also like to thank the characterization and support team of Pfizer that helped with powder analysis and continuous feedback on the project

I would like to thank the financial support provided by the Mitacs program that was funding in joint by Pfizer and Natural Sciences and Engineering Research Council of Canada (NSERC), and the University of Alberta.

Table of Content

List of Tables

List of Figures

Chapter 1: Introduction

1.1. Background

Therapeutic pharmaceuticals contain varying organic molecules, mixed with an array of excipients like sugars and buffer salts. Many pharmaceuticals, in liquid form, are prone to degradation mechanics that decrease the efficacy of the drug. Smaller organic materials, like antibiotics, experience chemical degradation by hydrolysis. Hydrolysis occurs when the organic molecule reacts with water, where the water is split into a hydroxyl group and a proton; both are bonded to separate parts of the broken organic molecule (Waterman, et al., 2002). Larger organic material, like proteins, have several potential hydrolysis sites but also experience physical degradation by unfolding and denaturing over time in a liquid solution (Waterman, et al., 2002; Manning, Chou, Murphy, Payne, & Katayama, 2010). Both degradation mechanisms have many factors, one factor common for both mechanisms is the solution's temperature; therefore, degradation can be slowed down at fridge temperature, but requires a cold chain for transportation (Manning, Chou, Murphy, Payne, & Katayama, 2010). Ertapenem, a carbapenem antibiotic, was stable for 30 minutes at room temperature, compared to being stable for 24 hours in refrigeration (Jain, Sutherland, Nicolau, & Kuti, 2014). In order to eliminate the effects of hydrolysis in antibiotics and denaturation in proteins, liquid pharmaceuticals can be freeze-dried into stable solid forms. If stored at low humidity, freeze-dried Ertapenem has less than 2.50% degradation from initial concentration after two years (Cielecka-Piontek, Zajac, & Jelinska, 2008). Freeze-drying can increase both the storage temperature and the shelf life of the pharmaceutical. A list of the benefits and shortfalls to each drying method is shown in Table 1.1.

There are a variety of freeze-drying process used, but the most common processing technique is lyophilization. Lyophilization is a three-step process. The drug formulation is frozen in a vacuum chamber at a steady cooling rate. The crystal structure, pore size, ice crystals, and other physical properties are dependent on the freezing rate (Haselet & Oetjen, 2018). A vacuum is applied to the frozen cake while the temperature is gradually brought up and held at a specific point to promote primary drying. During primary drying, the majority of the water in both the ice and freeze concentrate is sublimed out of the frozen cake. Primary drying occurs anywhere between 24 to 48 hours and is dependent on the drug formulation, vacuum pressure, and drying temperature (Tang & Pikal, 2004). During secondary drying, the temperature of the cake is

increased to remove the residual moisture in the frozen cake. The freeze-dried product from lyophilization is homogenous in color, cake depth, purity, and solid phase (Haselet & Oetjen, 2018). Conventional freeze-drying can be used to preserve a wide selection of pharmaceuticals; one study shows a higher survivability of a M13 model phage 60 days after freeze-drying compared to the liquid counterpart (Zhang, Peng, Zhang, Watts, & Ghosh, 2018). Although lyophilization can freeze-dry most drug formulations, it is an expensive and time-consuming process. A typical lyophilization batch process will take anywhere between 24 to 72 hours (Tang & Pikal, 2004). Vacuum chambers are expensive to operate and are energy intensive throughout the freeze-drying process (Trelea, Passot, Fonseca, & Marin, 2007). A freeze-dried formulation at higher mass concentration have low wetting properties (Cao, et al., 2013; Leuenberger H. , 2002).

An alternative to conventional freeze-drying is spray freeze-drying. Spray freeze-drying involves spraying the drug formulation into a freezing medium, like liquid nitrogen. The increased surface area in spray freeze-drying improves the dissolution rate and wetting properties of the cake produced (Yu, Johnston, & Williams III, 2006). Spraying the formulation into a cold medium causes instant freezing, which preserves the spherical shape of the droplets and reduces degradation mechanics present during phase separation in lyophilization (Heller, Carpenter, & Randolph, 1999). Although there is reduced degradation by eliminating phase separation present in lyophilization, there is an increase of protein aggregation at the air-liquid interface when atomizing the particles into a cryogenic fluid (Webb, Golledge, Cleland, Carpenter, & Randolph, 2002). The atomizing nozzle can increase pharmaceutical degradation therefore; the choice of the nozzle has significant impact on the process loss (Leung S. S., et al., 2016). The frozen particles are dried in similar fashion as conventional freeze-drying and have similar drying times in the order of days (Shoyele & Cawthorne, 2006).

Another alternative to conventional freeze-drying is spray drying. Spray drying, compared to freeze-drying, is a continuous drying process that has drying times, of similar mass, in the order of hours rather than days (Shoyele & Cawthorne, 2006; Kemp & Oakley, Modelling of particulate drying in theory and practice, 2002). The powders in spray drying are uniform and can be controlled to specific sizes based on the atomizing nozzle, feedstock flow rate, atomizing gas flow rate and drying temperature (Chegini & Chobadian, 2005). The size and aerodynamic characteristics of spray-dried powder makes it a suitable processing method for drugs intended for

pulmonary delivery (Matinkhoo, Lynch, Dennis, Finlay, & Vehring, 2011; Kemp, et al., 2013). Spray drying was shown to be a feasible process in preserving phages and having proper aerosolization characteristics for pulmonary delivery (Leung S. S., et al., 2016). Although spray drying is an efficient drying method, the temperature and process conditions required for spray drying is not suitable for some pharmaceuticals and biologics (Yoshii, et al., 2008; Morgan, Herman, White, & Vesey, 2006).

Atmospheric spray freeze-drying (ASFD) is an alternative to conventional freeze-drying that will be discussed in this work. ASFD began with the discovery that sublimation of water from a frozen sample is based on the relative pressure at the sublimation surface rather than the absolute pressure of the entire sample (Meryman, 1959). Instead of drying the sample in a vacuum chamber at low pressures and temperature, the sample can be dried at low temperatures with fast flowing gas that creates a relative vacuum pressure at the sample's surface. ASFD was later used in the food industry for freeze-drying liquid foods like juices, coffees, and teas (US Patent No. 3,313,032, 1967). A fluidized bed was utilized to increase the surface to air exposure between the drying gas and the frozen food droplets. A comparison between vacuum freeze-dried and ASFD food products show that ASFD produces a similar quality powder with lower processing time (Boeh-Ocansey, 1983). Mathematical models show that reducing particle size increases the surface mass transfer coefficient resulting in faster drying rates (Heldman & Hohner, 1974). ASFD increases the dissolution rate of drugs with low water solubility (Leuenberger H. , 2002). Vacuum freeze-dried drug formulation, with high mass concentration, has low solubility, but the increased surface area of ASFD improves the wetting properties of the dried product. A variation of the fluidized bed ASFD apparatus was developed by using concurrent drying gas flow and a gas jacket created by a porous tube to prevent sprayed particles adhering to the chamber (Wang, Finlay, Peppler, & Sweeney, 2006). In the variation ASFD apparatus, a model protein, bovine serum albumin, and a bacteria, *Bordetella pertussis* aivrulent strain BP347, had lower process degradation from ASFD than by lyophilization. ASFD creates homogenous and high quality powder with increased surface area that have excellent wetting properties (Mumenthaler & Leuenberger, 1991; Ishwarya, Anandharamakrishnan, & Stapley, 2015). Processing time for ASFD is in the order of hours compared to tray lyophilization, which is in the order of days (Wang, Finlay, Peppler, & Sweeney, 2006; Ishwarya, Anandharamakrishnan, & Stapley, 2015).

Table 1.1 Strengths and Weaknesses of each Drying Process

Drying Process	Lyophilization	Spray Freeze-Drying	Spray Drying	Atmospheric Spray Freeze-Drying
Strengths	Repeatable	Forms Porous Particles	Engineered Particles for Desired Characteristics	Forms Porous Particles
	Versatile (works on many formulations)	Stable Drying Process	Fast process	Fast Freeze-Drying Process
	Stable Process		Continuous Process	
Weaknesses	Long Drying Time	Long Drying Time	High Process Temperatures	Batch Process
	Batch Process	Batch Process	Losses due to Atomization	Losses due to Atomization
	Solubility Issues at High Concentrations	Losses due to Atomization		

1.2. Objective

The first objective of this study is to further characterize the ASFD process and determine the effects of changing the feedstock concentration on the dried powder. ASFD is similar to spray freeze-drying but with a shorter drying time and uses flowing gas rather than a vacuum environment to dry the frozen particles. The drying process mimics the temperature hold shown in lyophilization, and the current seven-hour drying process was developed to minimize drying time and produce stable powders. The feedstock concentration was varied to determine the effects liquid mass concentration has on the particle morphology and surface characteristic. Pharmaceuticals that are lyophilized at high mass concentration are expected to have lower wetting properties, but ASFD is a freeze-drying process that creates porous particles with high surface area. Ertapenem, a carbapenem antibiotic, and trehalose, a common protein stabilizer in freeze-drying, was freeze-dried at varying mass concentrations. Although no quantitative analysis of the density or surface area was performed, microscope images give qualitative data of the effect feedstock concentration has on the dried powder.

Another objective is to determine the stabilization capabilities of ASFD on a biologic that is sensitive to process and environmental conditions. Currently, it is known that ASFD is a viable

process for freeze-drying bacteria and protein, but has not been further studied for pharmaceutical products (Wang, Finlay, Peppler, & Sweeney, 2006). One objective would be to expand the number of pharmaceutics that can be properly freeze-dried with ASFD. Although a model protein, bovine serum albumin, was previously freeze-dried with ASFD, this study will explore a complex and sensitive biopharmaceutical, bacteriophages (phages). Phage D29 was freeze-dried with a stabilizing sugar, trehalose, and a bulking sugar, mannitol. The phages were freeze-dried with various trehalose and mannitol mass ratios at constant feedstock concentration with different drying duration. In order to determine the ASFD bioactivity process loss, plaque assay measurements were performed on the phage powders to determine the phage activity before and after ASFD. Raman spectroscopy and moisture content measurement were used to determine the solid phase properties of the phage powders to predict the stabilization capabilities of the sugars. Scanning electron microscopy was used to determine the particles formed at different mass ratios of trehalose and mannitol. It will be shown that phage D29 can be freeze-dried by ASFD with minimal process losses. A graphical abstract of the phage experiment is shown in Figure 1.1.

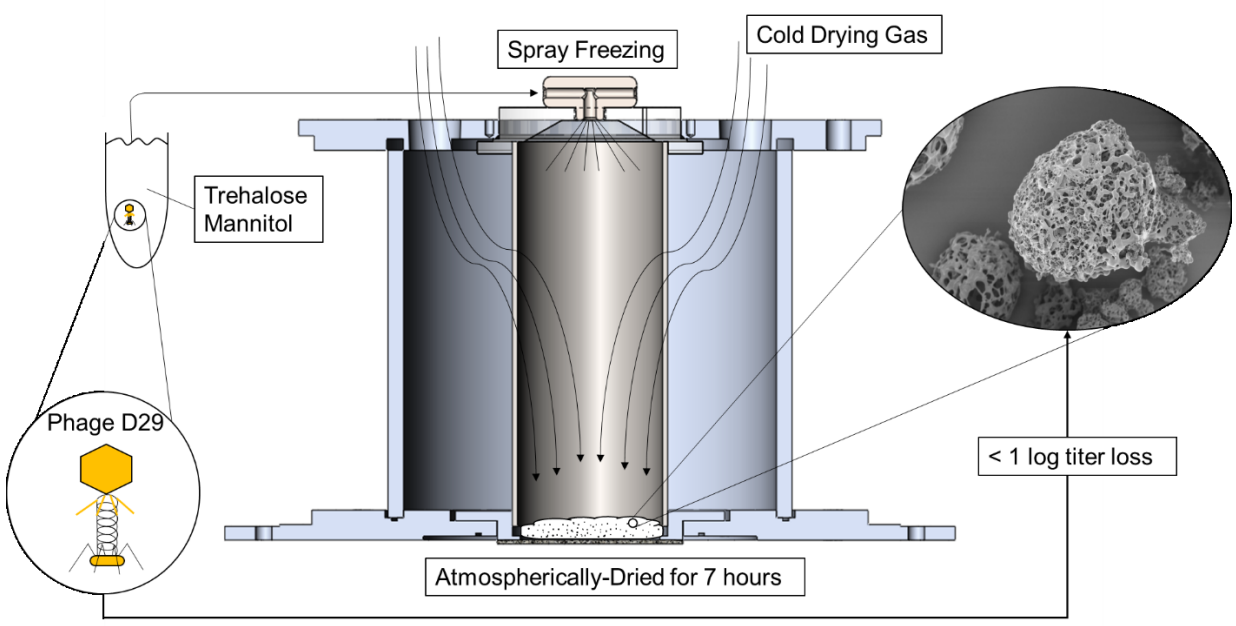

Figure 1.1 Graphical abstract of phage D29 experiment

1.3. Thesis Structure

The thesis is separated into two main chapters. The following chapter discusses the development of the ASFD process and the effects of changing the feedstock concentration on the dried powder. The description of the ASFD apparatus, operating procedure, and the changes in the ASFD apparatus is outlined in this chapter. Ertapenem is freeze-dried at various mass concentrations and compared with its lyophilized form. Ertapenem is used as a sample for current applications of ASFD. Trehalose, a common excipient in pharmaceutical formulations was also freeze-dried at varying feedstock concentration to determine the effects feedstock concentration has on the porosity, morphology, and size of the particles in the dried powder. Chapter 3 addresses work on using ASFD to stabilize phage D29. The phage freeze-drying experiment also present a viable formulation in using ASFD to preserve bacteriophages in a stable solid form. The phage activity loss, solid phase, moisture content, and SEM images of the powder is shown in this chapter and outline the potential for using this process in preserving phages in the future. Chapter 3 has been submitted for publication and is currently under review. The results in both chapters are summarized in the last section and a brief look on the limitations and future projects related to ASFD.

Chapter 2: Atmospheric Spray Freeze-Drying of Ertapenem, Trehalose, and the Effects of Feedstock Concentration

2.1. Introduction

Ertapenem is a parenteral carbapenem that has been approved for infection treatment since 2001 (Burkhardt, Derendorf, & Welte, 2007; Tice, 2004). Carbapenems are effective against a wide range of gram-positive and gram-negative bacteria making it a versatile class of antibiotics (Papp-Wallace, Ednimiani, Taracila, & Bonomo, 2011). Ertapenem has been often used as an outpatient antimicrobial therapy (OPAT) since it is an effective antibiotic that can be applied on a daily basis without patient discomfort (Teppler, et al., 2004). Although ertapenem is effective against many bacteria, it lacks long-term stability in liquid form (Tice, 2004). Jain *et al.* studied the stability of 100 mg/mL of ertapenem in syringes at varying storage temperatures (Jain, Sutherland, Nicolau, & Kuti, 2014). In that study, a solution was considered stable if it retained more than 90% of its initial concentration; therefore ertapenem solution was stable for 30 minutes at room temperature and 24 hours in refrigeration. One stabilization technique is to freeze-dry ertapenem into a solid dry form (Cielecka-Piontek, Zajac, & Jelinska, 2008). Cielecka-Piontek et al. demonstrated that the crucial degradation factor for solid ertapenem is the storage humidity. If the storage humidity was 0% RH, only 2.45% of the initial concentration of solid ertapenem will decompose after a 2-year period (Cielecka-Piontek, Zajac, & Jelinska, 2008).

Trehalose is a disaccharide commonly used for biologic stabilization. In its solid amorphous state, trehalose creates a glassy matrix that mechanically immobilizes the biologics and prevents potential destabilization mechanics in the biologics; this theory is known as the vitrification theory of freeze-drying (Jain & Roy, 2010; Mensink, Frijlink, Hinrichs, & van der Voort Maarschalk, 2017). Trehalose has a high glass transition temperature that allows it to remain in a solid amorphous state at room temperature, and is chemically inert, making it an ideal excipient for biologic stabilization (Wang W. , 2000). Trehalose can also chemically stabilize biologics by replacing the hydrogen bonds with the biologic; this chemical stabilization is effective in preventing proteins from denaturing (Jain & Roy, 2010; Mensink, Frijlink, Hinrichs, & van der Voort Maarschalk, 2017).

Lyophilization is the conventional freeze-drying method for pharmaceuticals. Lyophilization begins by freezing the liquid solution at a steady rate. The freezing rate effects the final product's crystal structure and size, porosity, and other physical properties (Haselet & Oetjen, 2018). The frozen solution is dried under vacuum at set temperatures throughout the process time. The process is complete when the freeze-dried cake has the desired moisture content. The freeze-dried product from lyophilization tend to be homogenous in color, cake depth, and purity (Haselet & Oetjen, 2018). The conventional freeze-drying process cover a wide selection of pharmaceutical solutions and have few limitations on what it can freeze-dry (Sadikoglu, Ozdemir, & Seker, 2006). Although tray lyophilization is a standard process in the pharmaceutical industry, there are several significant drawbacks to the process. In particular, it is a time consuming process where each batch of freeze-dried cake can take between 24 to 72 hours to complete (United States Patent No. 6,486,150 B2, 2002; Brulls & Rasmuson, 2002; Tang & Pikal, 2004). In addition, vacuum drying chambers are expensive to operate and require skilled technicians throughout the development and operation of the process (Trelea, Passot, Fonseca, & Marin, 2007). Finally, the dried cake produced can have low wetting properties (Cao, et al., 2013; Leuenberger H. , 2002).

Atmospheric spray freeze-drying (ASFD) is a process that involves spray freezing liquid droplets and drying at atmospheric pressures. The process consist of spraying a liquid solution into a cold chamber and instantaneously freezing the droplets. The frozen droplets are then sublimed with cold drying gas at varying temperatures through a 7-hour process. ASFD was first introduced by Meryman (1959), who showed that sublimation of ice was promoted by the relative vapor pressure gradient at the sample's surface rather than the absolute pressure; therefore, introducing a freeze-drying process outside of a vacuum environment (Meryman, 1959). ASFD was later utilized for food products where it was used to dry liquid foods like juices and teas (Malecki, Atmospheric Fluidized Bed Freeze Drying, 1970). Heldman and Hohner (1974) developed mathematical models for the ASFD process and determined that the reduction of particle size increased the surface mass transfer coefficient, therefore decreasing ASFD drying time (Heldman & Hohner, 1974). It was also shown that ASFD, compared to conventional freeze-drying, has the advantages of increased heat and mass transfer between the drying sample and the drying medium, high and homogenous quality of the dried product, and produces a free flowing powder with superior wetting properties (Ishwarya, Anandharamakrishnan, & Stapley, 2015; Mumenthaler & Leuenberger, 1991). Leuenberger (2007) expanded on this work and created a fluidized bed system

in freeze-drying a thermosensitive drug while improving the solubility of the drug (Leuenberger H. , 2002). An alternative of the ASFD apparatus was created by eliminating the fluidized bed and using concurrent flow to increase drying gas flow rate (Wang, Finlay, Peppler, & Sweeney, 2006). Wang *et al.* (2006) study showed that ASFD, compared to freeze-drying, caused lower degradation in protein and bacteria molecules (Wang, Finlay, Peppler, & Sweeney, 2006). This chapter explores the use of ASFD on freeze-drying ertapenem and trehalose at varying feedstock concentrations and the effects it has on the resultant dried powders.

2.2. Materials and Methods

2.2.1 Atmosphere Spray Freeze-Drying Apparatus

An existing ASFD apparatus used for experiments on bacteria and protein was modified for this research project (Wang, Finlay, Peppler, & Sweeney, 2006). A schematic of the modified ASFD apparatus is shown in Figure 2.1. The drying gas is supplied by a compressed air line connected to the building's air supply. The compressed air travels through a ½ - inch polycarbonate tube. Since the moisture of the compressed air is unknown, the compressed air first enters through a desiccator (Arrow Pneumatics D10-04, Broadview, IL, USA) that dries the compressed air via silica gel beads and exits the desiccator through a 40-micrometer filter. The dried compressed air is further cleaned by a 0.5-micrometer filter (Wilkerson AF1-04-S00, Richland, MI, USA). The compressed dry air travels through a compressed air regulator (Norgren R73G-2AK-RMN, BI, UK) where the pressure of the drying gas is reduced. The maximum dried air pressure is 500 kPa and is limited by the thickness of the atomizing gas tube. The dried air splits into two lines; one line supplies the twin fluid atomizer while the other line supplies the drying chamber with. The atomizer line passes through a rotameter (Cole Parmer, MTN, CAN) where the gas flow rate is controlled during the spray-freezing phase of ASFD. The drying chamber gas line is regulated by a control valve (Swagelok B-1RF4, OH, USA) and passes through a high-efficiency particulate air (HEPA) filter and then into a TSI flow meter (4043, Shoreview, MN, USA). The drying gas will then enter the heat exchanger through ½ - inch copper tubes.

The heat exchanger consists of coiled ½ -inch copper tubes and an upright steel chamber. The heat exchanger is cooled by spraying liquid nitrogen (Praxair, Edmonton, AB, CAN) into the steel chamber. The copper tube enters the top lid of the heat exchanger and coils down towards the bottom of the heat exchanger and back up to the lid of the heat exchanger. The coil increases contact between the surface of the copper tube and the liquid nitrogen. The copper tube exits the heat exchanger lid and enters the drying gas chamber. A heating rope (OMEGALUX FR-060, Laval, QC, CAN) insulates the intermediate tube between the heat exchanger and the drying chamber and is used to regulate the temperature of the drying gas.

The ASFD drying chamber has an aluminum outer cylindrical shell with an inner porous steel tube (Mott, Farmington, CT, USA). The inner porous steel tube creates a gas jacket that prevents the spray freeze droplets from adhering to the inside wall of the drying chamber and

directs the flow to the bottom of the drying chamber. The bottom of the drying chamber has a porous metal disc made of 316L stainless steel with a pore size of 20 micrometers (Applied Porous Technologies Inc., Tariffville, CT, USA). The top of the drying chamber has two bores for drying gas and a center bore for an acrylic adaptor that holds the twin fluid atomizer (Spray System Co. 1/8 JJCO, Wheaton, IL, USA). The acrylic adaptor can be altered for different nozzle size and types. The twin fluid atomizer has dry compressed air as the gas supply and a peristaltic pump (Chem-Tech CTPA4LSA, Punta Gorda, FL, USA) to supply the liquid feedstock.

The temperature is monitored by two Type T thermocouples. One thermocouple is placed in the drying chamber next to the filter on the outside of the porous tube. This thermocouple determines the temperature of the frozen powder throughout the process. The thermocouple cannot be placed inside the porous tube, as it will obstruct drying gas flow. Another thermocouple is placed directly under the porous filter where the frozen powder is collected and measures the temperature of the exit gas. The thermocouple in the drying chamber is connected to a temperature control system (OMEGA CN742, Laval, QC, CAN) that activates the rope heater. The temperature of the drying gas is increased by the rope heater and decreased by spraying additional liquid nitrogen into the heat exchanger. A humidity probe (Vaisala HMP75B, Woburn, MA, USA) with a hand held connector (Vaisala MI70, Woburn, MA, USA) is placed at the outlet of the drying chamber to determine the moisture of the outlet gas.

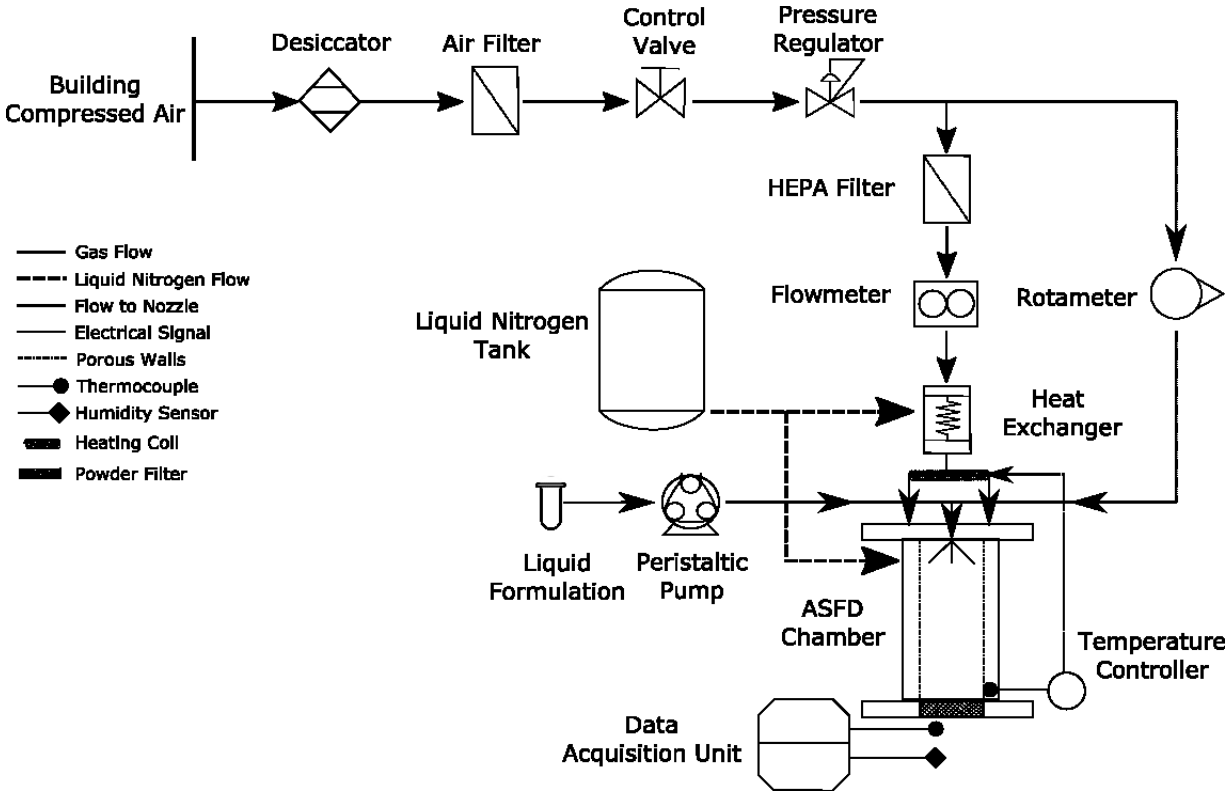

Figure 2.1 Schematic of ASFD apparatus.

2.2.2 Atmospheric Spray Freeze-Drying Process

The first stage in ASFD is the spray-freezing step. The drying chamber is first pre-cooled with liquid nitrogen for approximately 10 minutes. The drying chamber stabilizes at -130°C during the pre-cooling step. Dry gas is flowed through the drying chamber at 50 L/min. After pre-cooling, the feedstock is sprayed through a twin fluid nozzle with the liquid feed flowing at 20 mL/min and the air compressed air flowing at 10 L/min. At the end of the spray freezing stage, the drying chamber is warmed to -80°C.

The next stage in ASFD is the atmospheric drying step, which involves subliming the ice from the powder with desiccating gas at incremental temperature holds. After the frozen powder is collected on the filter, the drying gas flow increases to 150 L/min. The temperature of the drying gas is naturally brought up to -20°C within the first 20 minutes of atmospheric drying. The dry gas temperature is held constant at -20°C for two hours. The dry gas temperature is then raised to -15°C for one hour, then -10°C for one hour, then -5°C for one hour. After five hours, atmospheric drying is above water freezing temperature and it is assumed that the remaining water in the powder is entrapped in the freeze concentrate. The drying gas temperature is held at 5°C for an

additional hour. The drying gas temperature is naturally brought up to 25°C in the final hour of the drying process. The drying temperatures used in the process aimed to be below the glass transition temperature of the freeze concentrate throughout the process. A supplemented phase diagram was used as a guide to prevent glass transition of trehalose (Chen, Fowler, & Toner, 2000). The drying process is summarized in Table 2.1.

Table 2.1 ASFD operating procedure including drying gas flow rate and temperature

ASFD process step	Time (Minutes)	Drying Gas Flow (L/min)	Drying Gas temperature (°C)
Pre-Cooling	/	0	-130
Spray Freezing	0	50	-80
Atmospheric Drying	120	150	-20
	180	150	-15
	240	150	-10
	300	150	-5
	360	150	5
	420	150	25

2.2.3 Formulation Preparation

Tray lyophilized ertapenem cake (Batch 04143-139, Pfizer, New York City, NY, USA) was used for the ASFD experiments. The ertapenem solutions have varying mass concentrations of 50, 100, 150, and 200 mg/mL with a total volume of 10 mL. The tray lyophilized ertapenem cakes were reconstituted in water and passed through a 0.22-micron filter to extract any solid contaminants during reconstitution. The solution had yellow discoloration as the mass concentration of ertapenem increased. The mass concentration of ertapenem was restricted by its solubility limit. Feedstock concentrations higher than 200 mg/mL was not soluble at room temperatures and the feedstock was too viscous for the peristaltic pump.

D-(+)- trehalose dihydrate (T9531 ,St. Louis, MO, USA) powder was used for the trehalose component of the ASFD experiments. The trehalose had varying mass concentrations of 100, 200, and 300 mg/mL with a total volume of 10 mL. Trehalose was dissolved in water and passed through a 0.22-micron filter to extract undissolved solids.

2.2.4 Scanning Electron Microscope

A field emission scanning electron microscope (ZEISS Sigma FE-SEM, Oberkochen, DEU) was used to take images of each sample. An in-lens sensor and an excitation voltage of 3.0

kV was used to capture the microscopic images of ertapenem cake and powder. The samples were coated with a thin gold layer by using a Denton vacuum gold sputter unit (Desk 2, Moorestown, NJ, USA)

2.3. Results and Discussion

2.3.1 Improvements in ASFD Process

In the early stages of ASFD development, the drying gas was supplied from nitrogen gas bottles through a regulator into the ASFD system. The bottles were limited to 8400 liters of nitrogen gas per bottle. Bottled nitrogen gas was initially used because it is chemically inert and assumed dry. Two bottles of nitrogen gas, flowing at 80 L/min give a maximum of two hours of drying compared to the current seven-hour drying process at 150 L/min. Since two nitrogen gas bottles were previously used, the temperature of the drying chamber would dramatically increase when the nitrogen supply was switched from one bottle to the other. This gas supply switch created premature melting of the powder and a non-uniform quality of the dried powder. The limited drying gas and improper drying lead to the development of using compressed building air since the supply was nearly limitless and flowed at a steady and continuous rate. The concern with building air is contaminants and the moisture in the compressed air lines. The contaminants were removed by several filters in the system including a HEPA filter before contacting the drying gas. The moisture of the building compressed air is unknown but the desiccator in the system removes any remaining moisture.

The ASFD process used multiple temperature holds at varying temperatures. The initial temperature hold of -20°C was determined by copying the initial temperature hold used when tray lyophilizing ertapenem (United States Patent No. 6,486,150 B2, 2002). The subsequent temperature holds were determined by examining the moisture of the outlet drying gas. The humidity probe measures the water vapor density of the outlet gas, which is used as a qualitative indicator to determine when the mass and heat transfer in the powder have slowed significantly. The water vapor density is used to measure the moisture rather than the relative humidity. Since a majority of the ASFD process occurs at temperatures below 0°C, the relative humidity is large and does not directly represent the moisture of the outlet gas at low temperatures; therefore the water vapor density was used as an absolute measurement. After the water vapor density in the outlet gas has dropped and stabilized, the temperature of the drying gas was increased. The outlet gas temperature and water vapor density of an ASFD run can be shown in Figure 2.2. From the figure, it can be seen that raising the temperature from -20°C to -15°C temporarily raises the water vapor density, but every subsequent temperature increase has minimal effects on the moisture of the

outlet gas. Although this is not a direct way of measuring the moisture content of the powder, it is a simple technique used to develop the ASFD operating process.

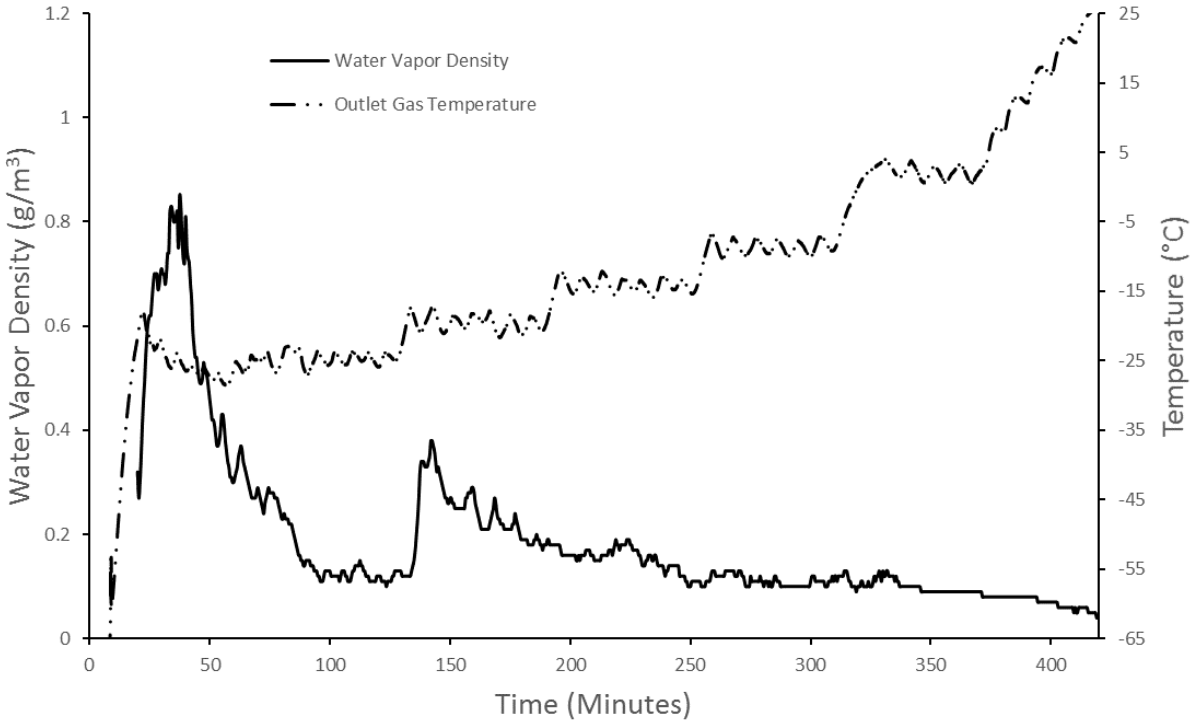

Figure 2.2 Typical ASFD run with outlet gas temperature and water vapor density.

2.3.2 Images of ASFD powder

Sample images of the ASFD powder on the filter is shown in Figure 2.3 and Figure 2.4. Figure 2.3 is trehalose powder from a feedstock with 100 mg/mL. From this image, it is seen that the powder is homogenous in color and is a free flowing powder. The powder is uniform around the center and tapers near the edge of the powder; this slope is caused by the flow mechanics of the ASFD apparatus. The combination of the flow rate and large outlet diameter creates a flow with low Reynold's number, calculated at 2590 and within the transitional flow regime. Therefore, it is hypothesized that the flow in the metal porous tube creates a Poiseuille flow regime and deposits more frozen droplets closer to the center of the filter and less at the edge of the filter. Figure 2.4 is ertapenem powder from 100 mg/mL feedstock. The powder has some discoloration similar to ertapenem dissolved in water at high concentrations. Ertapenem powder forms a cake rather than the free flowing powder seen with trehalose, but both powders are easily removed from

the porous metal filter. Figure 2.5 shows ASFD trehalose powders at three feedstock concentration in glass vials, from left to right, 100, 200, and 300 mg/mL. The 100 mg/mL powder is a free flowing powder with small solid cake-like pieces that is not distinguishable from the image. The 200 mg/mL powder forms solid cakes that are brittle and the round edges break into a powder upon applying pressure. The 300 mg/mL powder are solid brittle cakes with sharp edges and do not easily break apart to form powders.

Figure 2.3 ASFD trehalose powder at feedstock concentration of 100 mg/mL after removing from ASFD apparatus

Figure 2.4 ASFD ertapenem powder at feedstock concentration of 100 mg/mL after removing from ASFD apparatus

Figure 2.5 ASFD trehalose powder in glass vials. From left to right the powders feedstock concentration are 100, 200, and 300 mg/mL

2.3.3 Microscope Images of Ertapenem Powder

Scanning electron microscope (SEM) images were taken of the ASFD ertapenem powders. Figure 2.6 shows ertapenem powders at higher magnification. The left image is ASFD ertapenem at 50 mg/mL feedstock concentration. The particles are 10-20 micrometer in diameter and have large pores compared to the body of the particles. The right image is ASFD ertapenem at 200 mg/mL feedstock concentration. These particles are 60-70 micrometers in diameter with small pores compared to the body of the particle. Figure 2.7 shows ertapenem at lower magnification with the left image being eratpenem at 50 mg/mL and the right image being ertapenem at 200 mg/mL feedstock concentration. Ertapenem at lower concentration has smaller and more distinct particles that are spherical. At higher concentrations, ASFD ertapenem forms large agglomerates with individual particles larger than at lower feedstock concentrations. Sections of the high concentration ertapenem have sharp edges and flat faces similar to those seen in lyophilized ertapenem in the next figure. Figure 2.8 is an image of tray-lyophilized ertapenem. The particles in tray-lyophilized ertapenem are completely solid with flat surfaces and sharp edges. The lyophilized cake is speculated to have low wetting properties since it has lower specific surface area than the porous particles. From these SEM images, it is predicted that ASFD with higher feedstock concentration will produce larger particles with low void fraction compared to their lower concentration counterpart.

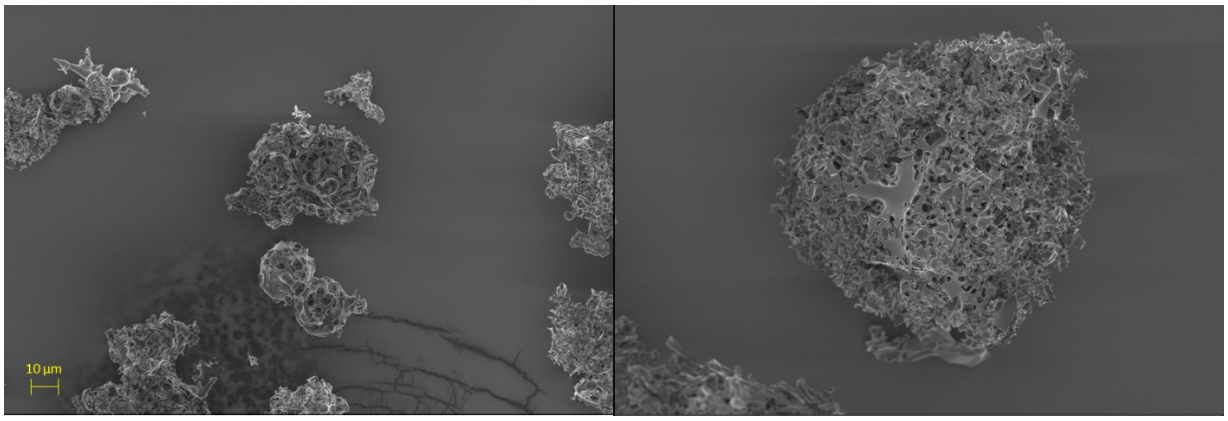

Figure 2.6 ASFD ertapenem powders at high magnification. Left image is trehalose at feedstock concentration of 50 mg/mL. Right image is trehalose at feedstock concentration of 200 mg/mL

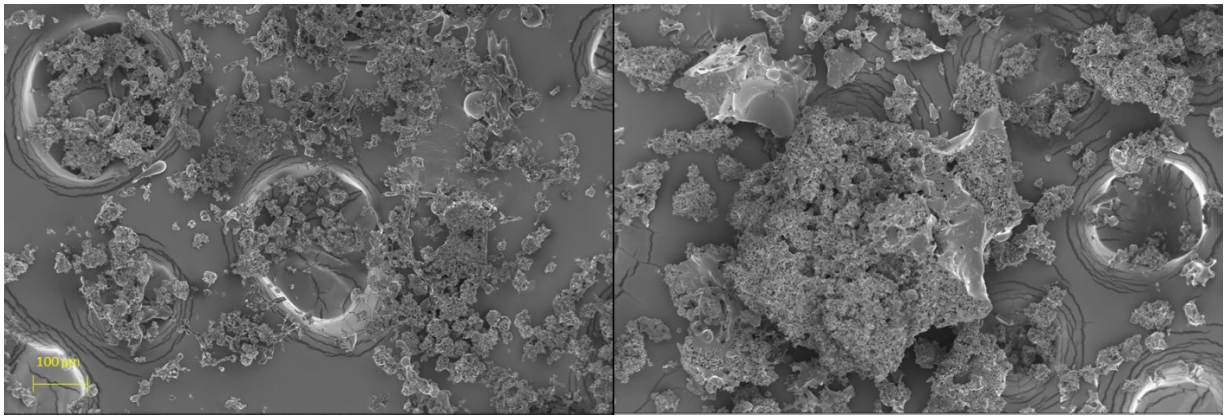

Figure 2.7 ASFD ertapenem powders at high magnification. Left image is trehalose at feedstock concentration of 50 mg/mL. Right image is trehalose at feedstock concentration of 200 mg/mL

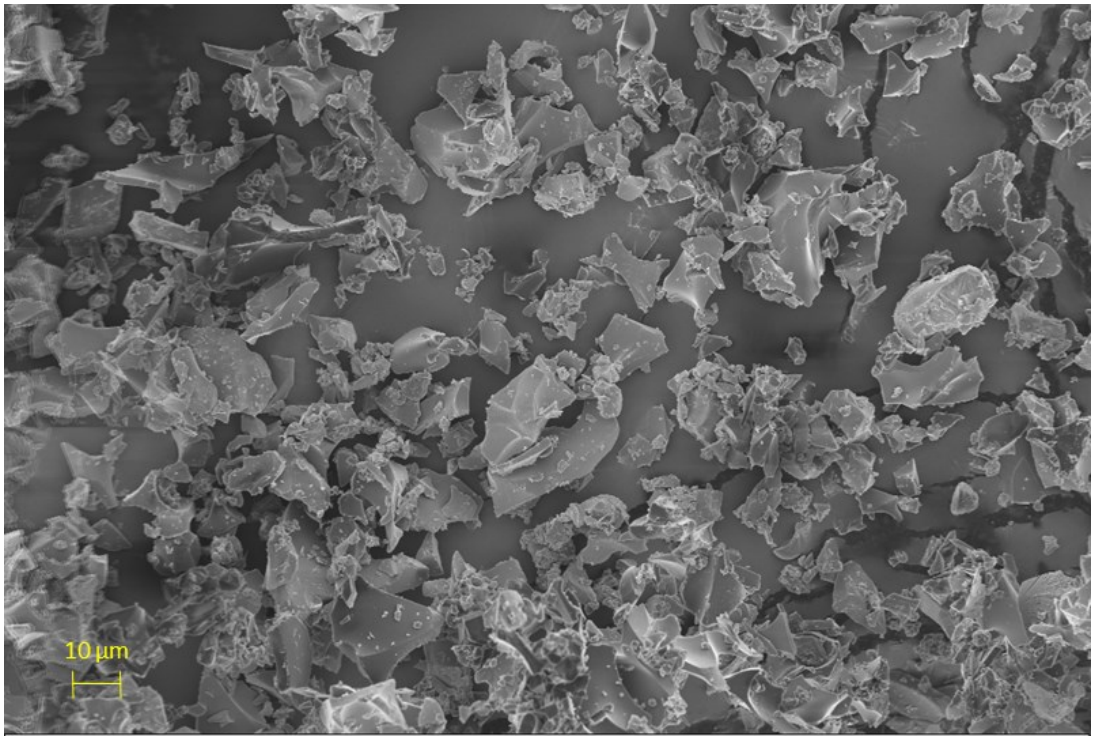

Figure 2.8 Tray lyophilized ertapenem powder

2.3.4 Microscope Images of Trehalose Powder

SEM images were taken of the ASFD trehalose powders. Figure 2.9 shows a high magnification image of trehalose powder particle for 100 mg/mL feedstock concentration powder on the left and 300 mg/mL feedstock concentration powder on the right. The particles on the left image, at lower feedstock concentration, appear to have thinner solid branches within the surface

of the particles; there are larger voids and more voids per particle, compared to the particles at three times the feedstock concentration. There are also many smaller distinct particles within 10 micrometers in the 100 mg/mL powder compared to the large agglomerated powder on the right. Figure 2.10 shows a group of trehalose powder particles for 100 mg/mL feedstock concentration powder on the left and 300 mg/mL feedstock concentration powder on the right. If the particles are approximated as spheres, two particles on the left image are close to 100 micrometers in diameter, while many particles are in the 20 to 30 micrometer range. The particles at higher feedstock concentration are at least 100 micrometers in diameter with few individual spherical particles. Figure 2.11 shows unprocessed D-(+)- trehalose dehydrate (trehalose). The unprocessed trehalose has sharp edges and flat faces with no voids; similar characteristics are seen in high feedstock trehalose particles. Although these images do not give a quantitative value for the powders' size distribution and porosity, it is a qualitative approximation of how feedstock concentration effects the powder. It is predicted that increasing feedstock concentration in ASFD will decrease the porosity of the particles and increase the size of the particles.

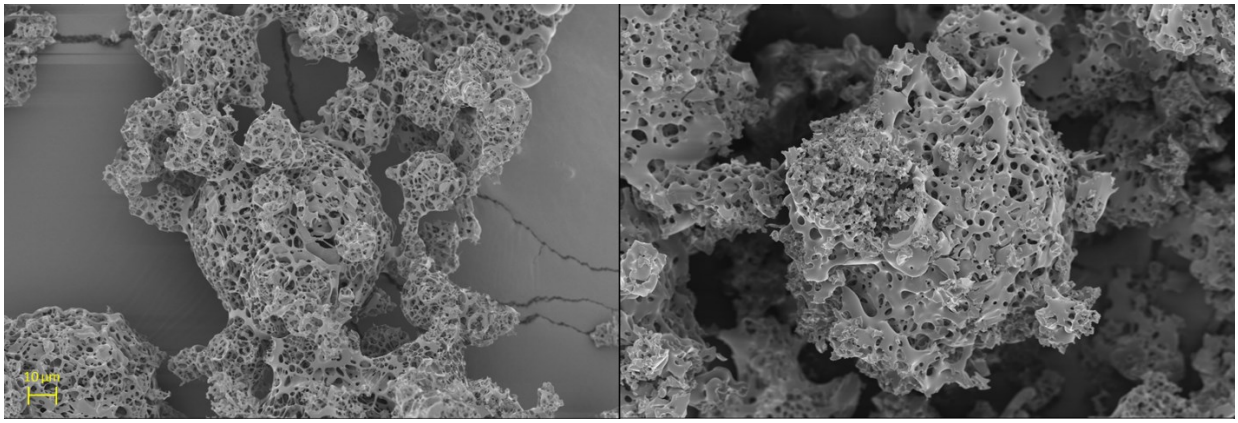

Figure 2.9 ASFD trehalose powders at high magnification. Left image is trehalose at feedstock concentration of 100 mg/mL. Right image is trehalose at feedstock concentration of 300 mg/mL

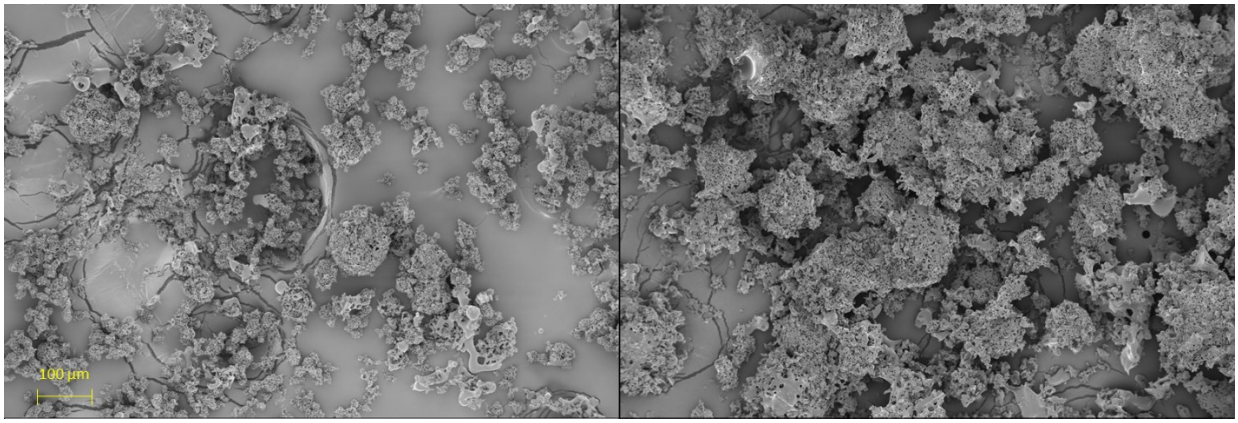

Figure 2.10 ASFD trehalose powders showing groups of particles. Left image is trehalose at feedstock concentration of 100 mg/mL. Right image is trehalose at feedstock concentration of 300 mg/mL

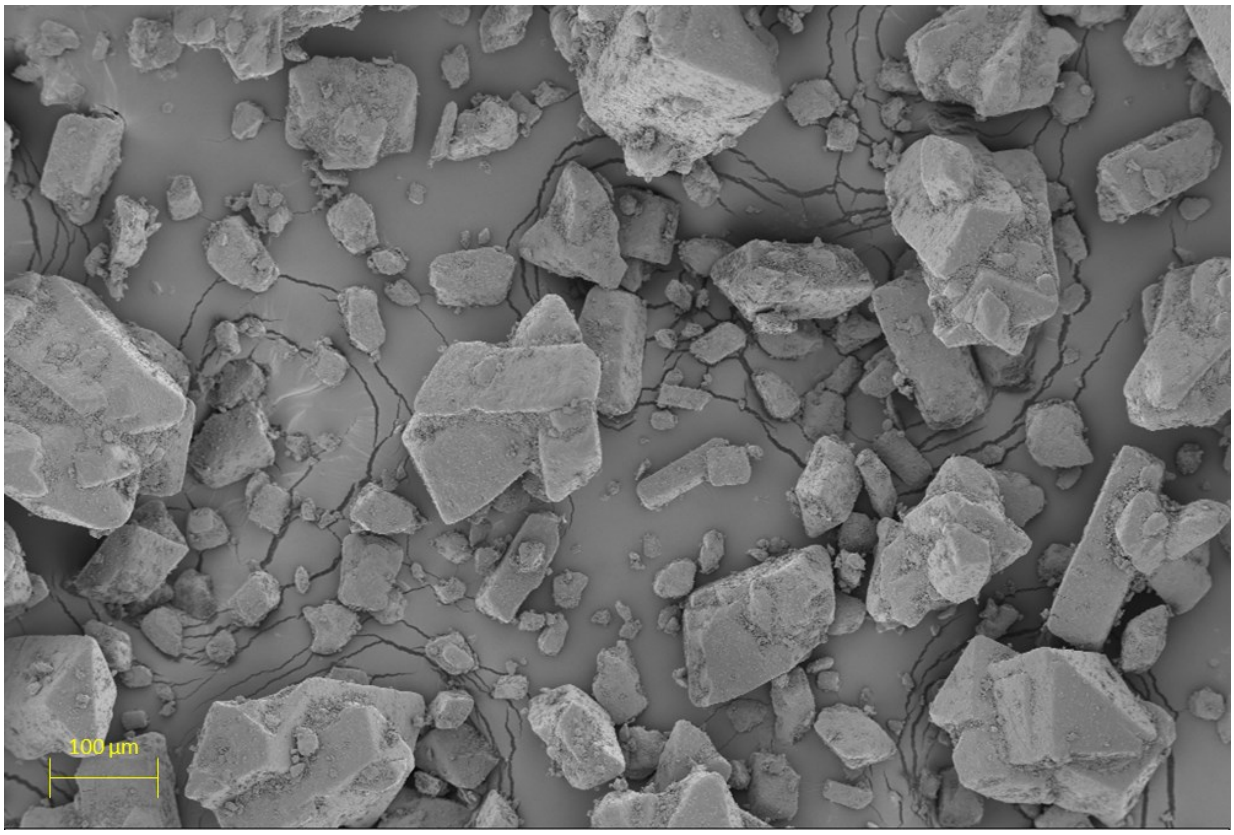

Figure 2.11 SEM images of unprocessed D-(+)- trehalose dihydrate

2.4. Conclusions

ASFD is a relatively new freeze-drying process that utilizes desiccating cold air to dry frozen powders with convective forces instead of vacuum forces in conventional freeze-drying. Ertapenem and trehalose were freeze-dried with ASFD at varying feedstock concentration. The freeze-dried particle characteristics can be altered by changing the feedstock concentration; higher feedstock concentration resulted in larger particles with lower porosity whereas lower feedstock concentration resulted in smaller particles high porosity. Using a low feedstock concentration, porous particles that have physical diameters of 20-30 micrometer can be formed that could have aerodynamic properties suitable for pulmonary delivery. Higher feedstock concentration can be used to create dense and large particles while having a processing time within hours compared to tray lyophilization, which have processing times of days. The current ASFD process significantly reduces the freeze-drying time while creating particles that are expected to have improved wetting properties; making it an attractive alternative to conventional forms of freeze-drying.

2.5. Chapter Citations

Brulls, M., & Rasmuson, A. (2002). Heat trasnfer in vial lyophilization. *Interational Journal of Pharmacetuics, 246*, 1-16.

Burkhardt, O., Derendorf, H., & Welte, T. (2007). Ertapenem: the new carbapenem 5 years after first FDA licensing for clinical practice. *Expert Opinion on Pharmacotherapy, 8*(2), 237-256.

Cao, W., Krishnan, S., Ricci, M. S., Shih, L.-Y., Liu, D., Gu, J. H., & Jameel, F. (2013). Rational design of lyophilized high concentration protein formulations-mitigating the challenge of slow reconstitution with multidisciplinary strategies. *European Journal of Pharmaceutics and Biopharmaceutics, 85*, 287-293.

Chen, T., Fowler, A., & Toner, M. (2000). Literature Review: Supplemented Phase Diagram of the Trehalose-Water Binary Mixture. *Cryobiology, 40*, 277-282.

Cielecka-Piontek, J., Zajac, M., & Jelinska, A. (2008). A comparison of the stability of ertapenem and meorpenem in pharmaceutical preparations in solid state. *Journal of Pharmaceutical and Biomedical Analysis, 46*, 52-57.

Haselet, P., & Oetjen, G.-W. (2018). 1. Foundations and Process Engineering. In *Freeze-Drying* (pp. 1-165). Weinheim: Wiley-VCH Verlag GmbH & Co. KGaA.

Heldman, D., & Hohner, G. (1974). An Analysis of Atmospheric Freeze Drying. *Food Sceince, 39*, 147-155.

Hunke, W. A., Illig, K. J., Kanike, A., Reynolds, S. D., Tsinontides, S. C., Al-Dehneh, A. S., & Patel, H. S. (2002, November 26). *United States Patent No. 6,486,150 B2.*

Ishwarya, S. P., Anandharamakrishnan, C., & Stapley, A. G. (2015). Spray-freeze-drying: A novel process for the drying of foods and bioproducts. *Trends in Food Science & Technology, 41*, 161-181.

Jain, J. G., Sutherland, C., Nicolau, D. P., & Kuti, J. L. (2014). Stability of ertapenem 100 mg/mL in polypropylene syringes stores at 25, 4, and -20°C. *American Jorunal of Health-System Pharmacy, 71*, 1480-1484.

Jain, K. N., & Roy, I. (2010). Trehalose and Protein Stability. *Current Protocols in Protein Science, 59*(4.9), 1-12.

Leuenberger, H. (2002). Spray Freeze-Drying - the process of choice for low water soluble durgs? *Jounral of Nanoparticle Research, 4*, 111-119.

Malecki, G. (1970). Atmospheric Fluidized Bed Freeze Drying. *Food Technology, 24*, 93-95.

Mensink, M. A., Frijlink, H. W., Hinrichs, W. L., & van der Voort Maarschalk, K. (2017). How sugars protect proteins in the solid state and during drying (review): Mechanisms of stabilization in relation to stress conditions. *European Journal of Pharmaceutics and Biopharmaceutics, 114*, 288-295.

Meryman, H. T. (1959). Sublimation Freeze-Drying without Vacuum. *Science, 130*, 628-629.

Mumenthaler, M., & Leuenberger, H. (1991). Atmospheric Spray-Freeze Drying: A Suitable Alternative in Freeze-Drying Technology. *International Journal of Pharmaceutics, 72*, 97-110.

Papp-Wallace, K. M., Ednimiani, A., Taracila, M. A., & Bonomo, R. A. (2011). Carbapenems: Past, Present, and Future. *Antimicrobial Agents and Chemotherapy, 55*(11), 4943-4960.

Pyne, A., Surana, R., & Suryanarayanan, R. (2002). Crystallization of Mannitol below Tg' during Freeze-Drying in Binary and Ternary Aqueous Systems. *Pharmaceutical Research, 19*(6), 901-908.

Sadikoglu, H., Ozdemir, M., & Seker, M. (2006). Freeze-drying of pharmaceutical products: research and development needs. *Drying Technology, 24*, 849-861.

Tang, X., & Pikal, M. J. (2004). Design of freeze-drying processes for pharmaceuticals: practical advice. *Phamraceutical Research, 21*(2), 191-200.

Teppler, H., Gesser, R. M., Friedland, I. R., Woods, G. L., Meibohm, A., Herman, G., . . . Isaacs, R. (2004). Safety and tolerability of ertapenem. *Journal of Antimicrobial Chemotherapy, 53*(2), 75-81.

Tice, A. D. (2004). Ertapenem: a new opportunity for outpatient parenteral antimicrobial therapy. *Journal of Antimicrobial Chemotherapy, 53*(2), ii83-ii86.

Trelea, I. C., Passot, S., Fonseca, F., & Marin, M. (2007). An interactive tool for the optimization of freeze-drying cycles based on quality criteria. *Drying Technology, 25*(5), 741-751.

Wang, W. (2000). Lyophilization and development of solid protein pharmaceuticals. *International Journal of Pharmaceutics, 203*, 1-60.

Wang, Z. L., Finlay, W. H., Peppler, M. S., & Sweeney, L. G. (2006). Powder Formation by Atmospheric Spray-Freeze Drying. *Powder Technology, 170*, 45-52.

Chapter 3: Atmospheric Spray Freeze-Drying of Sugar Solution with Phage D29

3.1. Introduction

With the recent emergence of multiple drug resistant bacteria, interest in therapeutic bacteriophage (phage) applications has increased. Phages present an alternative resource in combatting bacteria-related diseases (Kutateladze & Adamia, 2010). Phages are viruses that infect bacteria, and can have a narrow host range of target bacteria (Hatful & Vehring, 2016; Dewangan, Kashyap, & Giri, 2017). This narrow host range results in little to no off-target effects, unlike what is seen with conventional antibiotics, which often damage natural bacterial flora (Dewangan, Kashyap, & Giri, 2017; Loc-Carrillo & Abedon, 2011). Phages and antibiotics use different mechanisms in killing bacteria, so antibiotic resistant bacteria can remain vulnerable to killing by phages (Loc-Carrillo & Abedon, 2011). Although bacteria can develop resistance to phages, phages can mutate to overcome phage-resistance in the bacteria, and phage cocktails are commonly used to prevent resistance to one type of phage (Kutateladze & Adamia, 2010; Dewangan, Kashyap, & Giri, 2017; Loc-Carrillo & Abedon, 2011).

A phage structure generally consists of a polyhedral capsid containing genetic material and a tail used to bind to the bacteria and inject the genetic material (Hatful & Vehring, 2016; Dewangan, Kashyap, & Giri, 2017). Although not all phages can be used as therapeutic agents, lytic phages tend to be the most useful because of their exponential growth and effectiveness in eradicating the host bacteria (Kutateladze & Adamia, 2010). Unlike temperate phages, lytic phages have not been shown to transfer DNA between host bacteria, therefore eliminating the risk of spreading antibiotic or phage resistance genes (Loc-Carrillo & Abedon, 2011). Lytic phages operate by binding to and infecting host bacteria, multiplying within the host bacteria, and killing the host bacteria by rupturing the cell wall before releasing progeny and spreading to neighboring bacteria (Dewangan, Kashyap, & Giri, 2017).

One species of bacteria that exhibits multiple drug resistance is *Mycobacterium tuberculosis*, which in 2014 caused an estimated 480,000 cases of multi drug resistant tuberculosis, only half of which were successfully treated (World Health organization, 2018). There have also been cases of totally drug-resistant tuberculosis that can no longer be treated with any available antibiotics; therefore phage therapy is an interesting alternative treatment (Udwadia, 2016). While

each pathogen is susceptible to different strains of phages, for tuberculosis, *Mycobacterium* virus D29 is one of the most effective phages against this host (Hatful & Vehring, 2016; Guo & Ao, 2012; Lapenkova, Smirnova, Rutkevich, & Vladimirsky, 2018). Phage D29 are not only effective against tuberculosis, but are also safe to culture since they can be grown on *Mycobacterium smegmatis* rather than on *M. tuberculosis* (Hatful & Vehring, 2016). Liu *et al.* (2016) showed that inhalation of phage D29 resulted in a higher dose of phage D29 reaching and remaining in the lungs than did injection in mice (Liu, et al., 2016). Carrigy *et al.* (2017) compared the titer reduction in different inhalation devices for the delivery of phage D29 and found that titer reduction was highly dependent on the inhalation device, with the vibrating mesh nebulizer achieving the lowest titer reduction (Carrigy, et al., 2017).

In 2016, approximately 70% of new tuberculosis cases occurred in either Asia or Africa (World Health organization, 2018) in countries where a continuous cold-chain cannot always be guaranteed. In order to better utilize the potential of phage therapy in these regions, the development of phages in a dry solid form would be useful since phages, made of protein, are more susceptible to deactivation in liquid form than in a dry solid state (Wang W. , 2000). Therefore, it can be expected that a suitable dry dosage form would allow higher storage temperatures. The most common method of preserving proteins in a dry solid state is tray lyophilization (Wang W. , 2000). Zhang *et al*. (2018) successfully freeze-dried an M13KE model phage and showed that the phages had higher survivability as a dry powder than as liquid formulations for a storage period of 60 days; the dry powders were stored at room temperature whereas the liquid formulations were stored at 4°C (Zhang, Peng, Zhang, Watts, & Ghosh, 2018). Although there has been success in preserving phages with tray lyophilization, this technique is limited by cryoprotectant solubility and long processing times (Ishwarya, Anandharamakrishnan, & Stapley, 2015; Leuenberger H. , 2002). Spray drying is an alternative approach to preserving phages in a dry solid form. Although spray drying presents an attractive alternative with its faster processing time and ability to produce fine particles for inhalation, different phage strains are sensitive to different environmental and process conditions with the result that some phage species may demonstrate reduced viability after spray drying (Vandenheuvel, et al., 2013). Leung *et al.* (2016) examined the feasibility of both spray drying and spray freeze-drying of phages and the aerosolization characteristics of the resulting dry powders (Leung S. S., et al., 2016). Both processes resulted in similar overall titer reduction, which in the case of spray freeze-drying was caused mainly by the atomization step.

Atmospheric spray freeze-drying (ASFD) is a relatively new technique in protein preservation that offers an alternative to both spray drying and tray lyophilization. Meryman (1959) was the first to show that freeze-drying is based on the relative vapor pressure at the surface of the frozen object compared to the ambient pressure, rather than on the absolute vapor pressure, concluding that it is possible to freeze-dry without the use of a vacuum environment (Meryman, 1959). ASFD has improved mass and heat transfer rates, thereby decreasing drying time, giving high and homogenous quality to the dried product, and producing free-flowing powder with larger surface area and increased solubility (Ishwarya, Anandharamakrishnan, & Stapley, 2015; Mumenthaler & Leuenberger, 1991). Malecki *et al.* (1970) first used ASFD for liquid formulation in food products, specifically for the drying of liquid food and juices (Malecki, Atmospheric Fluidized Bed Freeze Drying, 1970). ASFD is also capable of freeze-drying thermosensitive pharmaceutical products that are difficult to properly dry in tray lyophilization (Wang, Finlay, Peppler, & Sweeney, 2006; Leuenberger, Plitzko, & Puchkov, 2006). Leuenberger (2002) developed a system to freeze-dry liquid pharmaceutical products using ASFD with a fluidized bed in a single freeze-drying chamber (Leuenberger H. , 2002). Wang *et al.* (2006) developed an ASFD system without a fluidized bed that succeeded in decreasing drying time and reducing the degradation of both proteins and bacteria formulations (Wang, Finlay, Peppler, & Sweeney, 2006). This paper explores the possibility of freeze-drying phage D29 with atmospheric spray freeze-drying.

3.2. Materials and Methods

3.2.1 Atmospheric Spray Freeze-Drying

An ASFD apparatus that improves upon the design given by Wang *et al.* (2006) was developed (Wang, Finlay, Peppler, & Sweeney, 2006). A schematic of the apparatus is shown in Figure 2.1. The drying gas is supplied by a building -compressed air line through a ½-inch polycarbonate tube. The compressed air first enters a desiccator (Arrow Pneumatics D10-04, Broadview, IL, USA) containing silica gel beads to dry the air prior to its exit through a 40-micron filter. The dry air is further cleaned by an additional 0.5-micron filter (Wilkerson AF1-04-S00, Richland, MI, USA). Pressure of the dry gas is reduced after the filter by a compressed air regulator (Norgren R73G-2AK-RMN, BI, UK). The dried and filtered compressed air splits into two lines. One line supplies atomizing gas to the twin-fluid nozzle with its flow rate controlled and measured by a rotameter (Cole Parmer, MTN, CAN). Drying gas supplied by the other line is regulated by a control valve (Swagelok B-1RF4, OH, USA) and then enters a HEPA filter connected to a TSI flow meter (4043, Shoreview, MN, USA). A coiled ½-inch copper tube is used to supply the drying gas through a heat exchanger that is filled with liquid nitrogen from a supply tank (Praxair, Edmonton, AB, CAN) to chill the drying gas. The heat exchanger is an upright sealed steel cylinder chamber. A heating rope (OMEGALUX FR-060, Laval, QC, CAN) is wrapped around the copper tube at the exiting end of the heat exchanger in order to heat the drying gas to designated operating temperatures.

The ASFD chamber consists of five main components: an aluminum top lid, a twin-fluid nozzle (Spray System Co. 1/8 JJCO, Wheaton, IL, USA), a porous metal cylinder (Mott, Farmington, CT, USA), an outer chamber, and a porous filter disc (Applied Porous Technologies Inc., Tariffville, CT, USA). The top lid has vent bores, a connector for liquid nitrogen filling, and connectors for copper tubing. The drying gas enters through the top lid and flows into the aluminum outer chamber. The porous cylinder is contained within the outer chamber and creates a gas buffer that prevents the sprayed particles from contacting the porous cylinder while directing the flow of particles to the filter disc. The twin-fluid nozzle is connected to the top lid. The nozzle has a gas supply from the compressed air line while the liquid is supplied by a peristaltic pump (Chem-Tech CTPA4LSA, Punta Gorda, FL, USA). The frozen powder is collected on the filter disc, which sits on an aluminum piece attached to the bottom of the ASFD chamber. The filter disc

is made of chemical and corrosion-resistant 316L Stainless Steel with a pore size of 20 micrometers.

A Type T thermocouple connected to a feedback system (OMEGA CN742, Laval, QC, CAN) that controls the heating rope was placed at the bottom of the ASFD chamber near the powder. Using the temperature near the powder, the heating rope warms the cold drying gas to the desired operating temperature. A similar thermocouple was placed at the exit of the ASFD chamber to measure the temperature of the outlet gas, which was recorded using a temperature logger (National Instrument USB-TC01, Austin, TX, USA). The humidity of the outlet gas was measured with a humidity probe (Vaisala HMP75B, Woburn, MA, USA) connected to a hand-held indicator (Vaisala MI70, Woburn, MA, USA).

3.2.2 Operating Procedure

The drying process was split into two main steps. The first step was the spray-freezing. The ASFD chamber was first cooled by pumping liquid nitrogen into the chamber while filtered and desiccated air flowed through the system. The chamber was cooled and upon stabilizing at -130 ° C, the liquid nitrogen was shut off and the phage solution was pumped through the twin-fluid nozzle. The liquid solution was pumped at 20 mL/min while the compressed air flowed through the nozzle at 10 L/min. At the end of spraying, the ASFD chamber had warmed to -80°C.

The second step in ASFD was atmospheric drying. This began by gradually increasing the temperature of the chamber from -80°C to -20°C. The drying gas temperature was regulated by the rope heater and the volume of liquid nitrogen in the heat exchanger. The chamber temperature was kept at -20°C for two hours and then held constant for one hour each at incrementally higher temperatures. The temperature was eventually brought up to 25°C. Since the water vapor density of the outlet gas was independent of the gas temperature, the vapor density instead of the relative humidity was used to determine the chamber temperature throughout the drying process. The water vapor density was used as a qualitative indicator to determine when the mass transfer of water from the powder had slowed or stopped completely. When the vapor density of the outlet gas decreased and reached a plateau, the temperature of the drying gas was increased. In order to lower the moisture content of the phage powder, the drying time was increased by one hour in the second set of phage powders. Figure 3.1 shows the water vapor density of the outlet gas and the drying chamber set temperature for a typical run.

The powder sample was collected by removing the filter at the end of the ASFD process. The samples were stored in plastic vials (Fisher-Scientific Eppendorf Tubes, Ottawa, ON, CAN) inside a drybox at 25°C. To study the effect of storage temperature, a portion of the powder samples was also stored in a drybox in the fridge at 4°C.

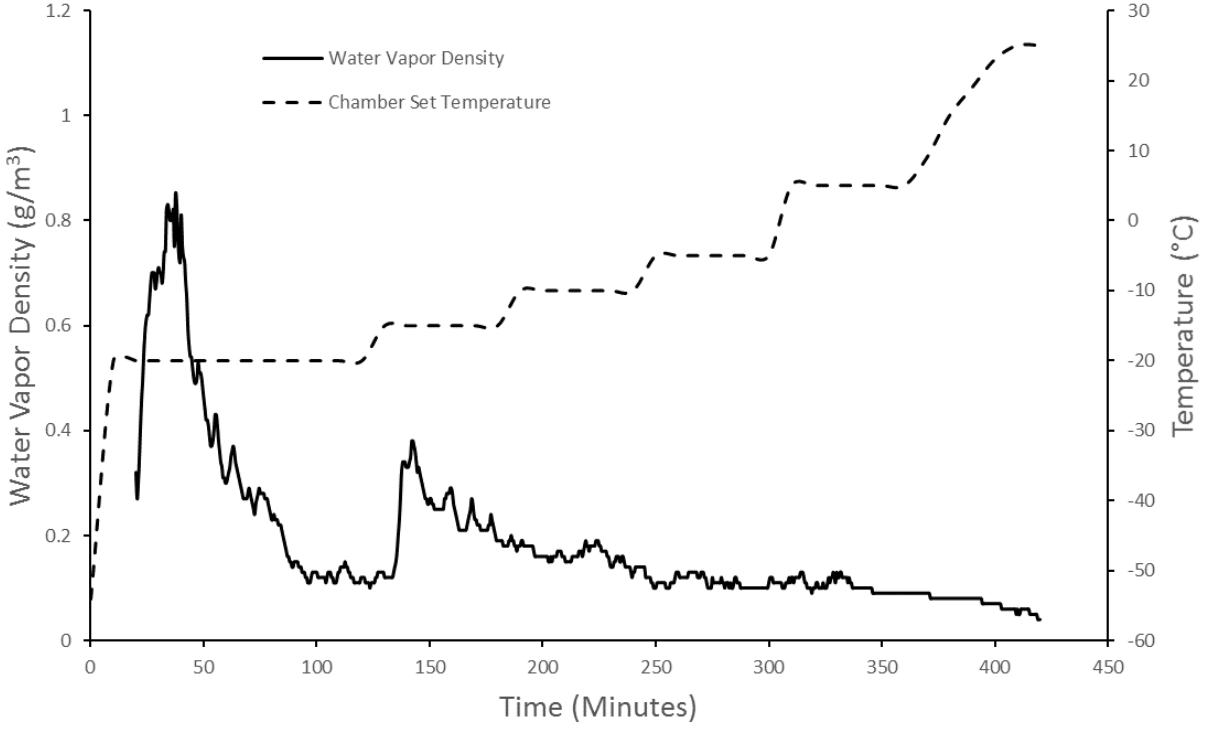

Figure 3.1: ASFD process development that correlates chamber set temperature and water vapor density of outlet gas. The solid black line corresponds to the water vapor density graph. The dashed line corresponds to the chamber set temperature. The water vapor density measurement starts 20 minutes into the run to accommodate the humidity probe's lower operating limit of -50°C.

3.2.3 Formulation Preparation

ASFD was used to produce powders with phage D29 using three formulations of varying trehalose and mannitol mass ratios, for a total mass concentration of 100 mg/mL. Table 3.1 shows the three formulations and two duplicate samples used to freeze-dry phage D29. For the A2 and B2 powders, the ASFD process was increased from a 6-hour drying process (for powders A, B, C) to a 7-hour drying process. The liquid formulation contained either trehalose or a mixture of trehalose and D-mannitol, with the addition of D29 phages to a concentration ranging from 5.2 to 1.5 x 10^{11} pfu/mL. The D-(+)- trehalose dihydrate (T9531 ,St. Louis, MO, USA) and D-mannitol were both purchased from Sigma-Aldrich (M4125 ,St. Louis, MO, USA). Trehalose and D-mannitol were dissolved in 10 mL of deionized water at the proper mass ratio and concentrations.

The solution was then passed through a filter with 0.22-µm pore size. A micropipette was used to add 50 µL of D29 phage at a concentration ranging from 5.2 to 1.5 x 10^{11} pfu/mL to the solution, which was then vortexed; 500 µL of the phage solution was separated for titer measurement of the liquid formulation while the remaining liquid solution was freeze-dried with the ASFD apparatus.

Table 3.1: Feed solution composition for atmospheric spray freeze-drying. The total mass concentration of trehalose and mannitol was 100 mg/mL for each case.

ASFD Feed Solution	Mass ratio (% w/w)		Volume (mL)	Process Time (min.)
	Trehalose	Mannitol		
A	100	0	10	360
B	70	30	10	360
C	50	50	10	360
A2	100	0	10	420
B2	70	30	10	420

3.2.4 Moisture Measurement

The residual moisture of the freeze-dried powder was measured gravimetrically by comparing the weight of the sample before and after oven drying. The mass of the ASFD powders was measured on a glass dish and placed in an isotherm oven (Fisher-Scientific Isotemp 280A, Hampton, NH, USA). 100 mg of each sample was heated to 100°C at 3.0 kPa absolute pressure for 8 hours and slowly cooled in the oven overnight. The vacuum oven was periodically vented and pumped to ensure that the air around the sample was dry.

3.2.5 Titer Measurement

Plaque assays on the surrogate host *M. smegmatis* mc^2155 were used to measure the titer of the phages in plaque-forming units per mL (pfu/mL). The prepared samples were in freeze-dried solid form and were resuspended in ~1 mL of phage buffer prior to plaque assay and the subsequent titer measurement. The full-plate titer method was used since the plaques were too large to use the spot assay method. Details of the plaque assay method are given elsewhere (http://www.bdbiosciences.com, n.d.).

3.2.6 Scanning Electron Microscope

Images of the resulting powders were taken using a field emission scanning electron microscope (ZEISS Sigma FE-SEM, Oberkochen, DEU). The images were taken with the

immersion lens detector at a working distance of 6.0 mm and an accelerating voltage of 3.0 kV. Each sample was coated with a 10 nm layer of gold prior to imaging using a Denton vacuum gold sputter unit (Desk 2, Moorestown, NJ, USA).

3.2.7 Raman Spectroscopy

A custom-designed dispersive Raman spectrometer was used for solid phase analysis of the dried powders. A 671 nm diode-pumped laser (Ventus 671, Laser Quantum, UK) with a maximum output power of 500 mW served as the excitation source. The powders were loaded into a conical cavity with a volume of 0.2 μL in an aluminum sample holder and kept under a nitrogen atmosphere during the measurement. All measurements were conducted at a temperature of 23 ± 1 °C and a relative humidity of less than 3%. Pure trehalose and its spray-dried form were measured respectively to obtain the spectra for crystalline and amorphous trehalose. Three polymorphic forms of mannitol, α, β, and δ, were also produced and measured for their Raman reference spectra. D-mannitol was tested directly as received and used as the reference for β-mannitol. The other two forms of polymorphs were prepared using a slow solvent evaporation method (Wang, Boraey, Williams, Lechuga-Ballesteros, & Vehring, 2014). Briefly, α-mannitol was obtained by adding D-mannitol to a mixed solvent of acetone, ethanol, and water in the volume ratio of 5:5:2 at 50°C during electromagnetic stirring and then cooling the solution down to room temperature to allow crystal precipitation. The δ-form of mannitol was achieved by drying the aqueous solution of D-mannitol at room temperature in a vacuum desiccator.

A deconvolution process (Wang, et al., 2017) was used to determine the contributions of each component in multi-component systems according to Eqn. (1)

$$S_{\mathrm{Res}} = S_{\mathrm{Raw}} - \left[B + \sum \left(I_i \pm e_i \right) S_{i,\mathrm{N}} \right] \quad (1)$$

in which S_{Res} is the residual spectrum after subtracting all components from the raw spectrum of the multi-component mixture, S_{Raw}, and B is the background signal. The normalized reference spectrum, $S_{i,\mathrm{N}}$, is used as the spectral intensity unit for the corresponding pure component, and the spectral contribution of the component to the raw spectrum of the mixture is $I_i S_{i,\mathrm{N}}$. The deconvolution approach was performed manually by iteratively adjusting the intensity factor, I_i, to minimize the residuals for each component. Uncertainty of the intensity factor for

each component, $\pm e_i$, is a range within which the corresponding component is no longer distinguishable between under- and over-subtraction. The intensity factors for each component are directly related to their corresponding mass fractions.

3.3. Results

3.3.1 Titer Measurement

The absolute titers of the phage measured for a) the phage lysate, b) the feedstock, i.e. the lysate mixed with sugar formulation, and c) the final freeze-dried powder of phages are shown in Figure 3.2. Figure 3.3 shows the titer reduction from feedstock preparation and the freeze-drying process using the initial titer as a reference. Trehalose and mannitol at a 1:1 mass ratio (powder C) had an unacceptably large titer reduction of ~ 3 logs, from the feedstock to the dried powder; therefore, feedstock for powder C was not used again. This result is consistent with previous phage research where lower mass ratios of trehalose correlated with lower phage survivability (Leung S. Y., et al., 2017). In both titer measurements of powder B and B2 with a trehalose-to-mannitol mass ratio of 7:3, the ASFD process showed a consistent titer reduction of the feedstock to the freeze-dried powder of ~0.8 and ~0.6 logs, respectively. The pure trehalose powder had high titer reductions of ~1.5 and ~4.0 logs, for powders A and A2, respectively.

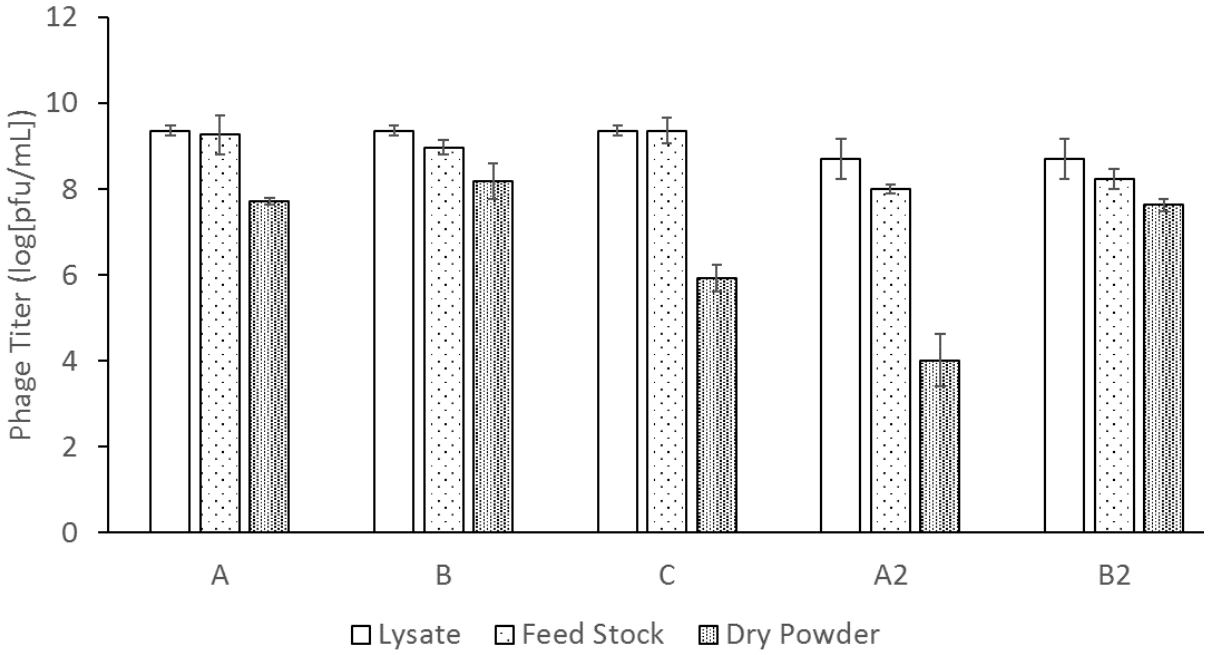

Figure 3.2: Phage titer measurement of the lysate, liquid solution, and dry powder for each solution

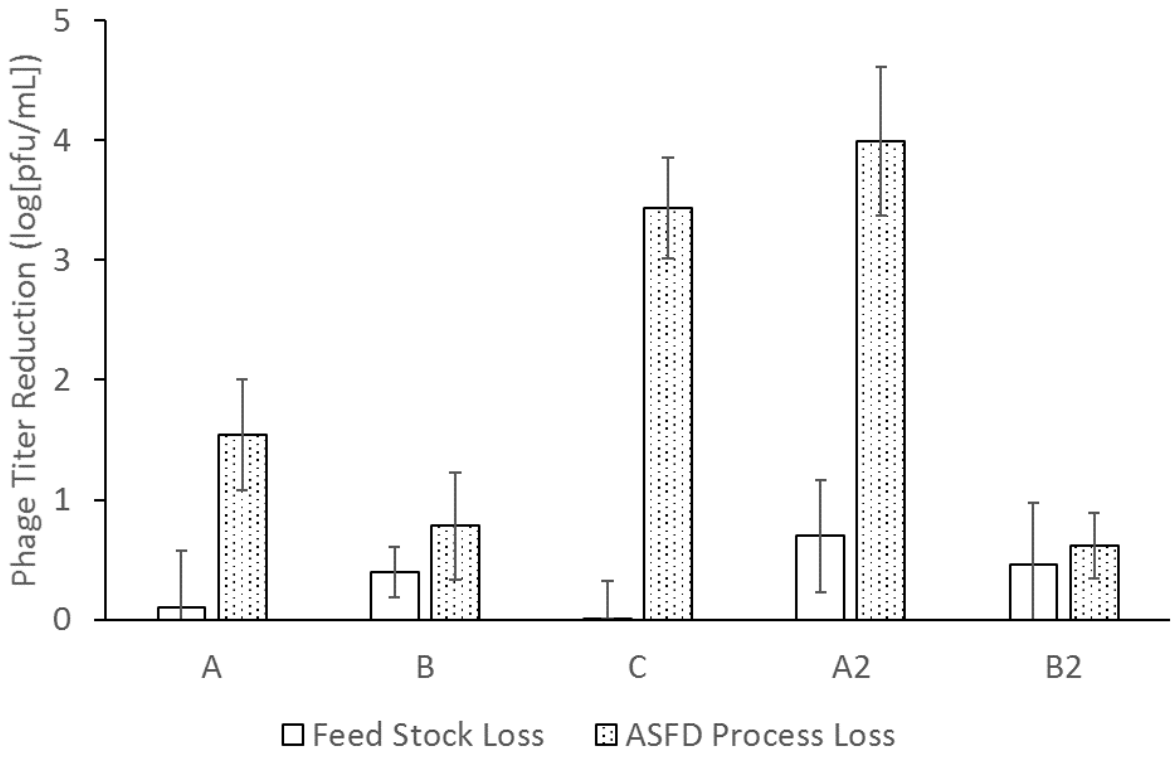

Figure 3.3: Phage titer loss occurring upon formulation and freeze-drying process for each solution

3.3.2 Moisture Content

The moisture contents of the ASFD powders are shown in Figure 3.4. The first batch (A) had two different storage conditions in order to determine the best short-term storage environment. One set of powder samples were stored in a drybox at room temperature (25 °C), while another set of powder was stored in a drybox in a refrigerator at 4 °C. Powder A had a moisture content of 6.2 ± 0.1% w/w when stored in a drybox at room temperature and a moisture content of 9.6 ± 0.1% w/w when stored in a drybox for one week in the fridge. Powder B had a moisture content of 5.2 ± 0.1% w/w when stored in the drybox and a moisture content of 6.2 ± 0.1% w/w when stored in the refrigerator. Because of the differences in moisture content and negligible effects on titer measurement, the duplicate phage powders (A2, B2) were stored only in a drybox at room temperature. The additional hour of drying time used with the duplicate runs (A2, B2) decreased the moisture content to 4.6 ± 0.1% w/w and 4.9 ± 0.1% w/w for powders A2 and B2, respectively.

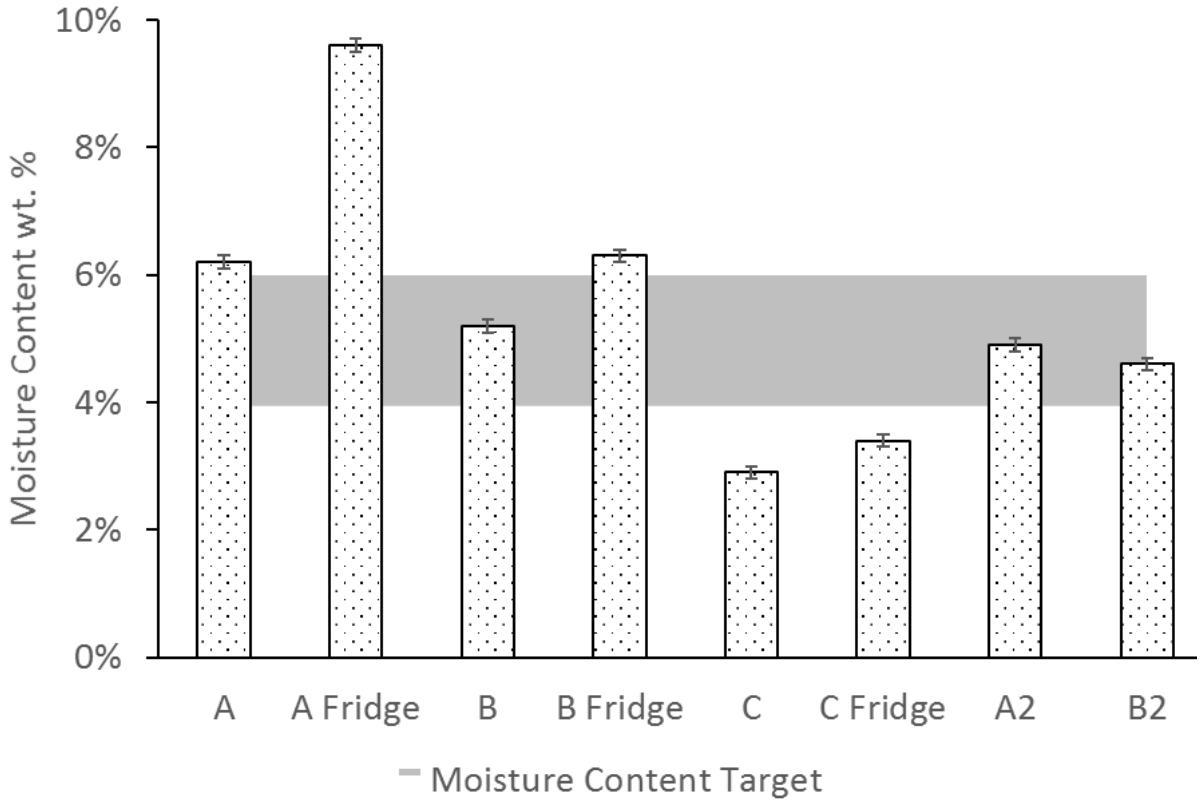

Figure 3.4: Moisture content of each powder stored in a drybox either at room temperature (25 °C) or in the fridge (4 °C). Shaded area (4%-6%) represents the ideal powder moisture content for phages.

3.3.3 Solid Phase Properties

The Raman spectra of the phage powders were obtained in order to determine the solid phase properties of the components in each powder. Powder A consisted only of trehalose, which remained completely amorphous. In powder B, a mixture of trehalose and mannitol, the trehalose remained amorphous, while the mannitol crystallized. The deconvoluted spectrum of powder B is shown in Figure 3.5. The spectral range for C-H bond stretching (2800-3000cm^{-1}) was used for the deconvolution process. Amorphous trehalose, $I_{\text{a-Tre}}S_{\text{a-Tre,N}}$, was identified as the dominant component in the raw spectrum for the large number of C-H bonds in its molecular structure compared to mannitol. Amorphous trehalose was therefore first subtracted from the raw spectrum, leaving the residual trace for mannitol component as $S_{\text{Raw}} - I_{\text{a-Tre}}S_{\text{a-Tre,N}}$, in which different polymorphs of mannitol, α, β, and δ, were detected. Characteristic peaks of different mannitol

polymorphs used for the deconvolution are marked in Fig. 6. A summed spectrum of all the deconvoluted components compared with the raw spectrum shows a good agreement, indicating that all components have been identified and their fractions properly quantified. The obtained intensity factors for each mannitol polymorph, $I_{\alpha\text{-M}}$, $I_{\beta\text{-M}}$, and $I_{\delta\text{-M}}$, were used directly to calculate the relative amount of each mannitol polymorph in powder B as $I_{\alpha\text{-M}}/(I_{\alpha\text{-M}}+I_{\beta\text{-M}}+I_{\delta\text{-M}})$, $I_{\beta\text{-M}}/(I_{\alpha\text{-M}}+I_{\beta\text{-M}}+I_{\delta\text{-M}})$, and $I_{\delta\text{-M}}/(I_{\alpha\text{-M}}+I_{\beta\text{-M}}+I_{\delta\text{-M}})$, respectively, as the quantification results show in Table 2. Field Emission Scanning Electron Microscope (SEM) images of the dried powders are shown in Figure 3.6. The images of powder A with 100% trehalose are shown in the left panels. The images of powder B, mixture of trehalose and mannitol solution, are shown in the right panels.

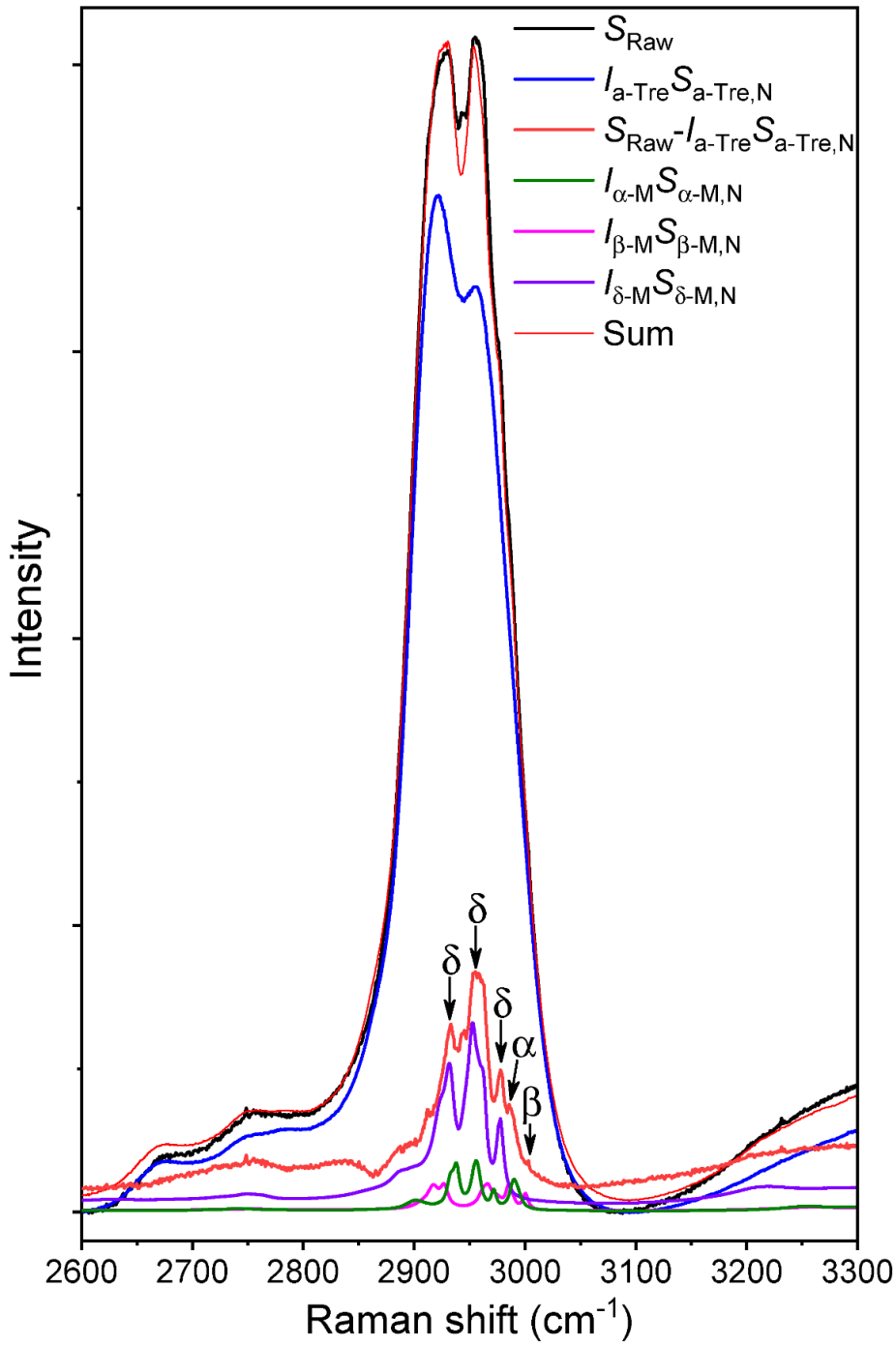

Figure 3.5: Deconvoluted Raman spectrum of ASFD powder with trehalose and mannitol at a mass ratio of 70:30. Spectral contributions of amorphous trehalose and three mannitol polymorphs (α, δ, β) were detected and separated from the raw mixture spectrum, leading to the sum of the deconvoluted components superimposed well within the measured spectrum.

Table 3.2 Crystal structures of sugars in phage powder

Sample	Trehalose	Mannitol		
		α	β	δ
Powder A	**amorphous**	-	-	-
Powder A2 (Replicate)	**amorphous**	-	-	-
Powder B	**amorphous**	15.4% ± 8.0%	15.4% ± 8.0%	69.2% ± 12.0%
Powder B2 (Replicate)	**amorphous**	19.1% ± 6.8%	10.6% ± 6.5%	70.2% ± 12.2%

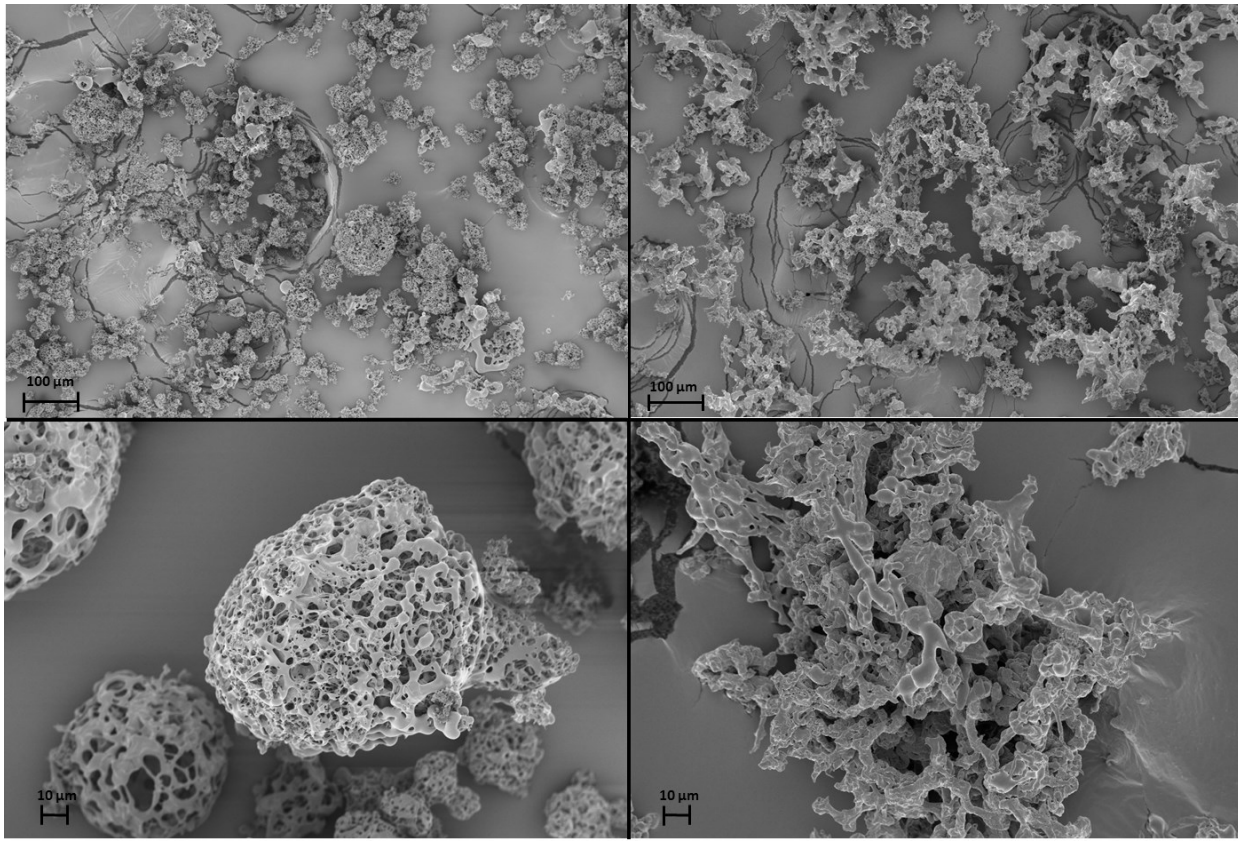

Figure 3.6: Scanning electron microscope (SEM) images of phage powders. Powder A, Trehalose powder, is shown in the left panels (top and bottom). Powder B, Trehalose-Mannitol powder, is shown in the right panels (top and bottom)

3.4. Discussion

Figure 3.3 shows that ASFD of phage D29 using trehalose and mannitol as excipients provides reasonable biological preservation of the phages during processing. Trehalose is a common disaccharide used for protein preservation since it has a high glass transition temperature, is chemically inert, and exhibits low hygroscopicity (Wang W. , 2000). When a protein is desiccated with amorphous trehalose as an excipient, trehalose is believed to immobilize the protein in a glassy matrix, hindering denaturization of the protein; this hypothesis is also known as the vitrification theory of freeze-drying (Jain & Roy, 2010; Mensink, Frijlink, Hinrichs, & van der Voort Maarschalk, 2017). The hydrogen in water molecules is generally assumed to form bonds with the protein to maintain its secondary structure, which can be affected by the removal of water. Trehalose may act as a replacement to water and create hydrogen bonds with the protein to confer stability (Jain & Roy, 2010; Mensink, Frijlink, Hinrichs, & van der Voort Maarschalk, 2017). Trehalose also has a high affinity to water and can act as a lyoprotectant. Water that is in contact with the trehalose bonded to the phage proteins may be forced into a conformation that prevents or delays ice formation (Jain & Roy, 2010), thereby inhibiting direct contact between the ice crystals and the phage particles. Recent studies have been conducted by Jain and Roy on the effectiveness of trehalose in preserving different types of proteins (Jain & Roy, 2010). The SEM images of powder A showed that the powder particles are porous and spherical in shape. The porous structure is formed when the solution freezes and ice crystals are formed that separate from the freeze concentrate. Many of the powder particles agglomerate. From the low magnification image (Figure 7, top left), it can be seen that the particles vary in size between 5 to 50 microns, which is attributed to the twin fluid atomizer that produces a polydisperse spray in this size range.

Mannitol is a commonly used excipient in tray lyophilization. As a crystalline bulking agent, mannitol, can prevent the collapse of a powder cake, which aids in drying at higher temperatures and acts as an excipient in preventing trehalose from crystallizing (Pyne, Surana, & Suryanarayanan, 2002; Krauss, Merlino, Vergara, & Sica, 2013). The effects of mannitol in the powder are seen from the comparison of the SEM images in Figure 3.6. The SEM images of powder B (right panels) show that the particles are porous but lack spherical structure and are larger than those of powder A (left panels). Although particles of both powders have a highly porous structure, the exclusion of mannitol in powder A leads to particles with rounder edges, a

sign of partial structure collapse. It is hypothesized that the addition of mannitol limits the particle collapse by creating a crystalline structure that stabilizes the particles.

The solid phase structure is an important powder characteristic as it indicates whether the powder matrix possesses the necessary stability to protect the phages during storage (Izutsu, Yoshioka, & Terao, 1993). Trehalose needs to remain in the form of an amorphous glass to protect the phages from stress during freezing and drying. Mannitol is expected to crystallize during the drying stage and form a supporting skeleton for the particles to prevent the structure from collapse. The propensity of mannitol to crystallize during normal spray drying has been studied by Chan et al. in the case of spray-dried binary mixtures of mannitol and salmon calcitonin (Chan, et al., 2004). Crystallized mannitol with a combination of different polymorphs was detected in formulations with high mannitol concentrations (> 50%), and polymorphic transformations were reported upon exposure to moisture during storage. In comparison, the ASFD freezing step involves a fast cooling process in which mannitol will likely precipitate in amorphous and hemihydrate forms first and subsequently transition to δ-mannitol polymorphs throughout the drying step (Cao, Xie, Krishnan, Lin, & Ricci, 2013). Kim *et al.* (1998) showed that a faster cooling rate of mannitol generally created more δ-polymorphs of mannitol, a result that agrees with those from solid state analysis by Raman spectroscopy (Kim, Akers, & Nail, 1998; Su, Jia, Li, Hao, & Li, 2017). Although δ-mannitol has lower stability than the commonly found β-polymorph, it has been reported to be stable for more than 3 years if stored at room temperatures (25 °C) and low humidity (Chan, et al., 2004; Burger, Henck, Rollinger, Weissnicht, & Stottner, 2000). The deconvoluted Raman spectra of powder B show that the trehalose remains in the amorphous state, which stabilizes the protein.

In the present study, a formulation with 7:3 trehalose to mannitol mass ratio (powder B) was found to provide the highest viability in the resultant dry powder after processing by ASFD. Because trehalose has a glass transition temperature of 16 °C at a moisture content of 9.6% (Chen, Fowler, & Toner, 2000), powder A (100% trehalose) is prone to crystallizing during storage at low temperatures when the moisture content remains constant. Crystallization of trehalose upon storage has been shown to reduce its cryoprotectant properties (Izutsu, Yoshioka, & Terao, 1993). The decrease in moisture content seen in Figure 3.4 for powders A2 and B2 increases the powder's glass transition temperature to 50 °C at a moisture content of 4.9% (Chen, Fowler, & Toner, 2000),

making the powder less prone to crystallization upon storage. Puapermpoonsiri (2010) showed that in their freeze-dried cakes containing phages, the optimal moisture content was in the range of 4-6% w/w, which is shown in the shaded region of Figure 3.4 (Puapermpoonsiri, Ford, & van der Walle, 2010).

The results of titer measurements are consistent with other freeze-drying studies that show that, at a proper ratio, trehalose and mannitol are suitable for lyoprotection and cryoprotection of phages (Zhang, Peng, Zhang, Watts, & Ghosh, 2018; Leung S. S., et al., 2016). Formulation for powder B had a titer loss of less than 1 log, which is an acceptable process loss for phages (Hoe, et al., 2013). The differences in titer loss between powder A and A2 is 2.5 logs, whereas the difference between powder B and B2 is 0.2 logs. It is hypothesized that this discrepancy between the original and duplicate runs is caused by the additional drying time in the latter. In order to lower the moisture content of the powder to an acceptable range, the drying time was increased and the moisture content of powder A was approximately halved.

The processing time for ASFD used in this study was approximately 7 hours to freeze-dry 10 mL of 100 mg/mL trehalose solution containing 10^9 pfu/mL of phages. A typical freeze-drying process time for tray lyophilization of a similar trehalose solution is approximately 3-5 days (Leung S. S., et al., 2016; Lu & Pikal, 2004). The difference in drying time can be attributed to the different drying mechanisms of each process. In ASFD, the solution is frozen nearly instantly upon spraying into the ASFD chamber. The quick freezing rate of the solution causes an even distribution of ice and freeze concentrate throughout the powder, therefore creating smaller ice crystals than with a slower freezing rate (Mumenthaler & Leuenberger, 1991). Both the water in the freeze concentrate and in the ice is removed via convection by the drying gas. As the ice mass on the particle surface decreases, the gas flow will have lower resistance to subliming the ice in the center of large particles (Wang, Finlay, Peppler, & Sweeney, 2006; Mumenthaler & Leuenberger, 1991). The drying mechanism creates a large specific surface area and particles that are porous without additional processes. In ASFD, the drying mechanism is dependent on the gas flow diffusing water out of the freeze concentrate and the ice; therefore, processing time can vary depending on the drying gas flow rate.

3.5. Conclusions

Results from the present freeze-drying experiments show that ASFD is a feasible method for preserving phage D29. Phages were stabilized with a mixture of trehalose-mannitol and freeze-dried in an ASFD apparatus with acceptable process losses. The phages were stored at room temperature in a drybox, but no long-term storage stability tests have been performed at this time. The preservation of phage D29 in this work indicates that the ASFD process is a promising candidate for powder production with phages that are sensitive to environmental conditions or that have a tendency to deactivate upon processing. The phage powders produced in ASFD show one possible formulation for stabilizing phage D29 in a solid form; but phage stabilization is dependent on other factors such as the feedstock solution, processing method, and type of phage. ASFD provided biological preservation similar to traditional methods but in a shorter processing time than conventional freeze-drying, making ASFD an attractive alternative method for preserving complex biological materials such as phages.

3.6. Chapter Citations

Burger, A., Henck, J.-O., Rollinger, J. M., Weissnicht, A. A., & Stottner, H. (2000). Energy/Temperature diagram and compression behavior of the polymorphs of D-mannitol. *Journal of Pharmaceutical Sciences, 89*(4), 457-468.

Cao, W., Xie, Y., Krishnan, S., Lin, H., & Ricci, M. (2013). Influence of process conditions on the crystallization and transition of metastable mannitol forms in protein formulations during lyophilization. *Pharmaceutical Research, 30*, 131-139.

Carrigy, N. B., Chang, R. Y., Leung, S. S., Harrison, M., Petrova, Z., Pope, W. H., . . . Vehring, R. (2017). Anti-Tuberculosis bacteriophage D29 Delivery with a vibrating mesh nebulizer, jet nebulizer, and soft mist inhaler. *Pharmaceutical Research, 34*, 2084-2096.

Chan, H.-K., Clark, A. R., Feeley, J. C., Kuo, M.-C., Lehrman, R. S., Pikal-Cleland, K., . . . Lechuga-Ballesteros, D. (2004). Physical stability of slamon calcitonin spray-dried powders for inhalation. *Journal of Pharmaceutical Sciences, 93*(3), 792-804.

Chen, T., Fowler, A., & Toner, M. (2000). Literature Review: Supplemented Phase Diagram of the Trehalose-Water Binary Mixture. *Cryobiology, 40*, 277-282.

Dewangan, G., Kashyap, D. K., & Giri, D. K. (2017). Bacteriophage and their Applications: A Review. *Journal of Cell and Tissue Research, 17*(2), 6165-6169.

Guo, S., & Ao, Z. (2012). Phages in the diagnosis and treament of tuberculosis. *Frontiers in Bioscience, 17*, 2691-2697.

Hatful, G. F., & Vehring, R. (2016). Respirable Bacteriophage Aerosols for the Prevention and Treatment of Tuberculosis. In *Drug Delivery Systems for Tuberculosis Prevention and Treatment* (pp. 277-292). John Wiley & Sons, Ltd.

Hoe, S., Semler, D. D., Goudie, A. D., Lynch, K. H., Matinkhoo, S., Finaly, W. H., . . . Vehring, R. (2013). Respirable Bacteriophages for the Treatment of Bacterial Lung Infections. *Journal of Aerosol Medicine and Pulmonary Drug Delivery, 26*(6), 317-335.

http://www.bdbiosciences.com. (n.d.). Retrieved August 7, 2018, from http://www.bdbiosciences.com/sg/resources/baculovirus/protocols/plaque_assay.jsp

Ishwarya, S. P., Anandharamakrishnan, C., & Stapley, A. G. (2015). Spray-freeze-drying: A novel process for the drying of foods and bioproducts. *Trends in Food Science & Technology, 41*, 161-181.

Izutsu, K.-i., Yoshioka, S., & Terao, T. (1993). Decrease Protein-Stabilizing Effects of Cryoprotectants Due to Crystallization. *Pharmaceutical Research, 10*(8), 1232-1237.

Jain, K. N., & Roy, I. (2010). Trehalose and Protein Stability. *Current Protocols in Protein Science, 59*(4.9), 1-12.

Kim, A. I., Akers, M. J., & Nail, S. L. (1998). The Physical State of Mannitol after Freeze-Drying: Effects of Mannitol. *Journal of Pharmaceutical Sciences, 87*(8), 931-935.

Krauss, I. R., Merlino, A., Vergara, A., & Sica, F. (2013). An Overview of Biological Macromolecule Crystallization. *Internation Journal of Molecular Sciences, 14*, 11643-11691.

Kutateladze, M., & Adamia, R. (2010). Bacteriophages as potential new therapeutics to replace or supplement antibiotics. *Trends in Biotechnology, 28*(12), 591-595.

Lapenkova, M. B., Smirnova, N. S., Rutkevich, P. N., & Vladimirsky, M. A. (2018). Evaluation of the efficiency of lytic mycobacteriophage D29 on the model of M. tuberculosis-infected macrophage RAW 264 cell line. *Bulletin of Experimental Biology and Medicine, 164*(3), 344-346.

Leuenberger, H. (2002). Spray Freeze-Drying - the process of choice for low water soluble durgs? *Jounral of Nanoparticle Research, 4*, 111-119.

Leuenberger, H., Plitzko, M., & Puchkov, M. (2006). Spray Freeze Drying in a Fluidized Bed at Normal and Low Pressure. *Drying Technology, 24*, 711-719.

Leung, S. S., Parumasivam, T., Gao , F. G., Carrigy, N. B., Vehring, R., Finlay, W. H., . . . Chan, H.-K. (2016). Production of Inhalation Phage Powders Using Spray Freeze Drying and Spray Drying Techniques for Treatment of Respiratory Infections. *Pharmaceutical Research, 33*, 1486-1496.

Leung, S. Y., Parumasivam, T., Gao, F. G., Carter, E. A., Carrigy, N. B., Vehring, R., . . . Chan, H.-K. (2017). Effects of Storage Conditions on the Stability of Spray Dried, Inhalable Bacteriophage Powders. *International Journal of Pharmaceutics, 521*, 141-149.

Liu, K.-y., Yang, W.-h., Dong, X.-k., Cong, L.-m., Li, N., Li, Y., . . . Li, J.-s. (2016). Inhalation study of mycobacteriophage D29 aerosol for mice by endotracheal route and nose-only exposure. *Journal of Aerosol Medicine and Pulmonary Drug Delivery, 29*(5), 393-405.

Loc-Carrillo, C., & Abedon, S. T. (2011). Pros and Cons of Phage Therapy. *Bacteriophage, 1*(2), 111-114.

Lu, X., & Pikal, M. J. (2004). Freeze-Drying of Mannitol-Trehalose-Sodium Chloride-Based Formulations: The Impact of Annealing on Dry Layer Resistance to Mass Transfer and Cake Structure. *Pharmaceutical Development and Technology, 9*(1), 85-95.

Malecki, G. (1970). Atmospheric Fluidized Bed Freeze Drying. *Food Technology, 24*, 93-95.

Mensink, M. A., Frijlink, H. W., Hinrichs, W. L., & van der Voort Maarschalk, K. (2017). How sugars protect proteins in the solid state and during drying (review): Mechanisms of stabilization in relation to stress conditions. *European Journal of Pharmaceutics and Biopharmaceutics, 114*, 288-295.

Meryman, H. T. (1959). Sublimation Freeze-Drying without Vacuum. *Science, 130*, 628-629.

Mumenthaler, M., & Leuenberger, H. (1991). Atmospheric Spray-Freeze Drying: A Suitable Alternative in Freeze-Drying Technology. *International Journal of Pharmaceutics, 72*, 97-110.

Puapermpoonsiri, U., Ford, S., & van der Walle, C. (2010). Stabilization of bacteriophage during freeze drying. *Interational Journal of Pharmaceutics, 389*, 168-175.

Pyne, A., Surana, R., & Suryanarayanan, R. (2002). Crystallization of Mannitol below Tg' during Freeze-Drying in Binary and Ternary Aqueous Systems. *Pharmaceutical Research, 19*(6), 901-908.

Su, W., Jia, N., Li, H., Hao, H., & Li, C. (2017). Polymorphism of D-mannitol: Crystal structure and the crystal growth mechanism. *Chinese Journal of Chemical Engineering, 25*, 358-362.

Udwadia, Z. F. (2016). Totally drug resistant-tuberculosis in India: The bad just got worse. *Journal of Association of Chest Physicians, 4*(2), 41-42.

Vandenheuvel, D., Singh, A., Vandersteegen, K., Klumpp, J., Lavigne, R., & Van den Mooter, G. (2013). Feasibility of spray drying bacteriophages into respirable powders to combat pulmonary bacterial infections. *European Journal of Pharmaceutics and Biopharmaceutics, 84*, 578-582.

Wang, H., Barona, D., Oladepo, S., Williams, L., Hoe, S., Lechuga-Ballesteros, D., & Vehring, R. (2017). Macro-Raman spectroscopy for bulk composition and homogeneity analysis of multi-component pharmaceutical powders. *Journal of Pharmacetuical and Biomedical Analysis, 141*, 180-191.

Wang, H., Boraey, M. A., Williams, L., Lechuga-Ballesteros, D., & Vehring, R. (2014). Low-Frequency Shift Dispersive Raman Spectroscopy for the Analysis of Respriable Dosage Forms. *International Journal of Pharmaceutics, 469*, 197-205.

Wang, W. (2000). Lyophilization and development of solid protein pharmaceuticals. *International Journal of Pharmaceutics, 203*, 1-60.

Wang, Z. L., Finlay, W. H., Peppler, M. S., & Sweeney, L. G. (2006). Powder Formation by Atmospheric Spray-Freeze Drying. *Powder Technology, 170*, 45-52.

World Health organization. (2018, February 15). Retrieved August 3, 2018, from http://www.who.int/en/news-room/fact-sheets/detail/antimicrobial-resistance

World Health organization. (2018, February 16). Retrieved August 3, 2018, from http://www.who.int/news-room/fact-sheets/detail/tuberculosis

Zhang, Y., Peng, X., Zhang, H., Watts, A. B., & Ghosh, D. (2018). Manufacturing and ambient stability of shelf freeze dried bacteriophage powder formulations. *International Journal of Pharmaceutics, 542*, 1-7.

Chapter 4: Conclusions

4.1. Summary of Work

The first objective of this thesis is to develop an Atmospheric Spray Freeze-Drying (ASFD) apparatus and operating process to freeze-dry ertapenem and trehalose; also, to determine the effects of the feedstock concentration on the dried powder. ASFD is a two-step process that involves spray freezing a feedstock into a cold drying chamber and drying the frozen powder with desiccating gas. The original ASFD apparatus was modified by including a PID controller for temperature adjustments and a humidity probe to develop an operating procedure for ASFD (Wang, Finlay, Peppler, & Sweeney, 2006). The ASFD apparatus has an improved gas system that utilize compressed air that is regularly available and treated to proper operating conditions. ASFD uses temperature holds based on the starting temperature of a typical lyophilization process and the moisture of the outlet gas. A decrease in the moisture of the outlet gas is an indicator of slowed mass and heat transfer and used as a qualitative indicator to increase the temperature of the ASFD process. ASFD is a seven-hour drying process for ertapenem, which normally takes 72 hours to dry with conventional freeze-drying (United States Patent No. 6,486,150 B2, 2002). Ertapenem at 50, 100, 150, and 200 mg/mL feedstock concentration was freeze-dried with ASFD and compared to the lyophilized counterpart. Scanning electron microscope (SEM) images indicated that ertapenem at higher feedstock concentrations produced smaller and fewer voids in the dried powder. It is predicted that ASFD improves the surface area of ertapenem compared to the lyophilized product thereby improving the wetting properties of the final product. Trehalose at 100, 200, and 300 mg/mL feedstock concentration was freeze-dried with ASFD. Trehalose powders, at lower feedstock concentration, produced free flowing powders that are spherical and have less agglomerated particles. Trehalose at higher feedstock concentration produced a brittle cake with large agglomerated particles. The current ASFD process can be used for biologic preservation and the desired powder characteristics are dependent on the feedstock concentration.

The second objective of this work is to determine the stabilization capabilities of ASFD on a bacteriophage (phage), which is a biologic that is difficult to preserve in a solid state. Phage D29 is a lytic phage known for its potency in infecting *Mycobacterium* tuberculosis. Phage D29 was freeze-dried using ASFD with varying ratios of treahlose and mannitol as stabilizing excipients. From chapter 2, a lower feedstock concentration produced smaller particles with higher porosity;

therefore, 100 mg/mL feedstock concentration was used for freeze-drying phage D29. Three ratios of trehalose to mannitol was used in this work and consisted of all trehalose, a 1:1 mass ratio of trehalose and mannitol, and 7:3 trehalose to mannitol mass ratio. The feedstock with 7:3 mass ratio led to the lowest titer reduction of ~0.6 logs, and had a powder moisture content of 4.9 ± 0.1%. The solution with all trehalose and 1:1 mass ratio of trehalose and mannitol had titer reductions greater than 1.5 logs. Raman spectroscopic analysis showed that the trehalose in the powder remained amorphous and the mannitol completely crystallized throughout the ASFD process; both solid phase are ideal characteristic for preserving phages and storage stability.

ASFD is shown to be a potential freeze-drying process for preserving biologics. Although not all parameters have been closely studied, the feedstock concentration has an effect on the powder's physical characteristics in terms of particle size and porosity. Feedstock concentration is one of many parameters that can be changed in the ASFD process with other parameters discussed in the next section. Freeze-drying of phage D29 shows the potential of preserving complex biologics with minimal losses. ASFD can be expanded to other biologics that are sensitive to environmental conditions or biologics that tend to deactivate upon processing. ASFD has shorter drying times than conventional freeze-drying with similar stabilization properties, making it an attractive alternative method for preserving biologics.

4.2. Future Work

This section will discuss some of the current limitations in the ASFD apparatus and the potential for future projects in developing the ASFD apparatus and process. The current ASFD process can stabilize a variety of biologics, which include bacteria, proteins, bacteriophages, and antibiotics, but could also be applied to other chemicals prone to decomposition in liquid form. Although a variety of pharmaceutical ingredients can be freeze-dried, the current operating process is tailored through trial and error for ertapenem, and bacteriophage D29 mixed with stabilizing sugars. These two examples display the potential for ASFD, but the current process may not be suitable for other biologics. Different strains within the same class of pharmaceutics may require a slower drying process or can handle an aggressive and faster drying process.

At the time of this manuscript submission, samples of ertapenem have been sent to labs to perform high performance liquid chromatography (HPLC) to determine the purity of the samples, Brunauer-Emmett-Teller (BET) surface area analyzer, to determine the specific surface area of the powder, and X-ray diffraction, to determine the crystal structure of the ertapemen powder. Although these tests have not been completed, the analysis of the purity, surface area, and crystal structure will be important in future ASFD experiments.

This project has also only showed one apparatus with one operating process, but many of the parameters in the process have significant effects on the powder characteristics. The current twin fluid atomizer used in the ASFD apparatus has not been characterized, therefore the droplet diameter distribution, dependent on the feedstock concentration, feedstock flow rate, and atomizing gas flow rate, have not been determined. As shown previously, the feedstock concentration have significant effects on the porosity and morphology of the final powder (Kim, Akers, & Nail, 1998; Yu, Johnston, & Williams III, 2006). Characterizing the current atomizer or using an already characterized atomizer would improve the control of the powder characteristics. The current ASFD process is set at seven hours with a drying gas flow rate of 150 L/min. The effects of changing the drying gas flow rate and the resultant powder characteristics and process time have not been investigated; further research can determine the optimal drying conditions. There could be a limit where increasing the drying gas flow rate, at a certain point, will have negligible effects on the process time. It is also possible that higher drying gas flow rate will create additional drying stress on the powder, which could cause a collapse in the particle's porous

structure. The chamber temperature has been set at the same temperature prior to spraying in all ASFD experiments. The freezing rate of the sprayed particles have effects on both the porosity and the crystal structure of the powder (Kim, Akers, & Nail, 1998). The effects of a faster or slower freezing rate and the resultant powder characteristics have yet to be explored. A faster freezing rate will create smaller and more abundant ice crystals whereas a slower freezing rate will create fewer and larger ice crystals (Mumenthaler & Leuenberger, 1991).

The current ASFD process is an estimated process developed with a predicted starting temperature hold of -20 °C. The starting temperature was an estimate based on ertapenem lyophilization process (United States Patent No. 6,486,150 B2, 2002). Each subsequent temperature hold was determined by the vapor density of the outlet drying gas. Water vapor density was chosen instead of relative humidity, since relative humidity is dependent on both the temperature and moisture of the outlet gas, whereas water vapor density is an absolute value. When the water vapor density of the outlet gas decrease and plateau, it is predicted that the heat and mass transfer of water from the freeze concentrate and ice in the powder has slowed. This is when the temperature is increased and held for a set time. The current ASFD process was developed through trial and error but is not suitable for different pharmaceuticals, particle size, and excipients in the feedstock. A real-time measurement technique could be used to determine the moisture of the powder throughout the process and the drying gas temperature can be increased to the glass transition temperature. Drying the powder at the glass transition temperature would have the highest mass and heat transfer of water from the freeze concentrate and ice to the drying gas while maintaining a desirable crystal structure in the stabilizer (Tang & Pikal, 2004). A near infrared (NIR) sensor or a Raman spectroscopy detector can be used to detect the moisture content of the powder. Using the moisture content, the glass transition temperature can be calculated and used for drying. This system would also need an automatic cooling system that is connected to the PID temperature controller. The current set up requires manual addition of liquid nitrogen to cool the drying gas, whereas a thermocouple connected to the PID temperature controller automatically warms the gas if the drying gas is below a set temperature. The sprayed powder, regardless of formulation and particle size, could be dried at optimal temperatures if both of these systems were implemented.

Bibliography

Boeh-Ocansey, O. (1983). A Study of the Freeze Drying of some Liquid Foods in Vacuo and at Atmospheric Pressure. *Drying Technology, 2*(3), 389-405.

Brulls, M., & Rasmuson, A. (2002). Heat trasnfer in vial lyophilization. *Interational Journal of Pharmacetuics, 246*, 1-16.

Burger, A., Henck, J.-O., Rollinger, J. M., Weissnicht, A. A., & Stottner, H. (2000). Energy/Temperature diagram and compression behavior of the polymorphs of D-mannitol. *Journal of Pharmaceutical Sciences, 89*(4), 457-468.

Burkhardt, O., Derendorf, H., & Welte, T. (2007). Ertapenem: the new carbapenem 5 years after first FDA licensing for clinical practice. *Expert Opinion on Pharmacotherapy, 8*(2), 237-256.

Cao, W., Krishnan, S., Ricci, M. S., Shih, L.-Y., Liu, D., Gu, J. H., & Jameel, F. (2013). Rational design of lyophilized high concentration protein formulations-mitigating the challenge of slow reconstitution with multidisciplinary strategies. *European Journal of Pharmaceutics and Biopharmaceutics, 85*, 287-293.

Cao, W., Xie, Y., Krishnan, S., Lin, H., & Ricci, M. (2013). Influence of process conditions on the crystallization and transition of metastable mannitol forms in protein formulations during lyophilization. *Pharmaceutical Research, 30*, 131-139.

Carrigy, N. B., Chang, R. Y., Leung, S. S., Harrison, M., Petrova, Z., Pope, W. H., . . . Vehring, R. (2017). Anti-Tuberculosis bacteriophage D29 Delivery with a vibrating mesh nebulizer, jet nebulizer, and soft mist inhaler. *Pharmaceutical Research, 34*, 2084-2096.

Chan, H.-K., Clark, A. R., Feeley, J. C., Kuo, M.-C., Lehrman, R. S., Pikal-Cleland, K., . . . Lechuga-Ballesteros, D. (2004). Physical stability of slamon calcitonin spray-dried powders for inhalation. *Journal of Pharmaceutical Sciences, 93*(3), 792-804.

Chegini, G. R., & Chobadian, B. (2005). Effect of spray-drying conditions on physical properties of orange juice powder. *Drying Technology, 23*(3), 657-668.

Chen, T., Fowler, A., & Toner, M. (2000). Literature Review: Supplemented Phase Diagram of the Trehalose-Water Binary Mixture. *Cryobiology, 40*, 277-282.

Cielecka-Piontek, J., Zajac, M., & Jelinska, A. (2008). A comparison of the stability of ertapenem and meorpenem in pharmaceutical preparations in solid state. *Journal of Pharmaceutical and Biomedical Analysis, 46*, 52-57.

Dewangan, G., Kashyap, D. K., & Giri, D. K. (2017). Bacteriophage and their Applications: A Review. *Journal of Cell and Tissue Research, 17*(2), 6165-6169.

Guo, S., & Ao, Z. (2012). Phages in the diagnosis and treament of tuberculosis. *Frontiers in Bioscience, 17*, 2691-2697.

Haselet, P., & Oetjen, G.-W. (2018). 1. Foundations and Process Engineering. In *Freeze-Drying* (pp. 1-165). Weinheim: Wiley-VCH Verlag GmbH & Co. KGaA.

Hatful, G. F., & Vehring, R. (2016). Respirable Bacteriophage Aerosols for the Prevention and Treatment of Tuberculosis. In *Drug Delivery Systems for Tuberculosis Prevention and Treatment* (pp. 277-292). John Wiley & Sons, Ltd.

Heldman, D. R., & Hohner, G. A. (1974). An Analysis of Atmospheric Freeze Drying. *Journal of Food Science, 39*, 147-155.

Heller, M. C., Carpenter, J. F., & Randolph, T. W. (1999). Protein formulation and lyophilization cycle deisgn: Prevention of damage due to freeze-concentration induced phase separation. *Biotechnology and Bioengineering, 63*(2), 166-174.

Hoe, S., Semler, D. D., Goudie, A. D., Lynch, K. H., Matinkhoo, S., Finaly, W. H., . . . Vehring, R. (2013). Respirable Bacteriophages for the Treatment of Bacterial Lung Infections. *Journal of Aerosol Medicine and Pulmonary Drug Delivery, 26*(6), 317-335.

http://www.bdbiosciences.com. (n.d.). Retrieved August 7, 2018, from http://www.bdbiosciences.com/sg/resources/baculovirus/protocols/plaque_assay.jsp

Hunke, W. A., Illig, K. J., Kanike, A., Reynolds, S. D., Tsinontides, S. C., Al-Dehneh, A. S., & Patel, H. S. (2002, November 26). *United States Patent No. 6,486,150 B2.*

Ishwarya, S. P., Anandharamakrishnan, C., & Stapley, A. G. (2015). Spray-freeze-drying: A novel process for the drying of foods and bioproducts. *Trends in Food Science & Technology, 41*, 161-181.

Izutsu, K.-i., Yoshioka, S., & Terao, T. (1993). Decrease Protein-Stabilizing Effects of Cryoprotectants Due to Crystallization. *Pharmaceutical Research, 10*(8), 1232-1237.

Jain, J. G., Sutherland, C., Nicolau, D. P., & Kuti, J. L. (2014). Stability of ertapenem 100 mg/mL in polypropylene syringes stores at 25, 4, and -20°C. *American Jorunal of Health-System Pharmacy, 71*, 1480-1484.

Jain, K. N., & Roy, I. (2010). Trehalose and Protein Stability. *Current Protocols in Protein Science, 59*(4.9), 1-12.

Kemp, I. C., & Oakley, D. E. (2002). Modelling of particulate drying in theory and practice. *Drying Technology, 20*(9), 1699-1750.

Kemp, I. C., Wadley, R., Hartwig, T., Cocchini, U., See-Toh, Y., Gorringe, L., . . . Ricard, F. (2013). Experimental study of spray drying and atomization with a two-fluid nozzle to produce inhalable particles. *Drying Technology, 31*(8), 930-941.

Kim, A. I., Akers, M. J., & Nail, S. L. (1998). The Physical State of Mannitol after Freeze-Drying: Effects of Mannitol. *Journal of Pharmaceutical Sciences, 87*(8), 931-935.

Krauss, I. R., Merlino, A., Vergara, A., & Sica, F. (2013). An Overview of Biological Macromolecule Crystallization. *Internation Journal of Molecular Sciences, 14*, 11643-11691.

Kutateladze, M., & Adamia, R. (2010). Bacteriophages as potential new therapeutics to replace or supplement antibiotics. *Trends in Biotechnology, 28*(12), 591-595.

Lapenkova, M. B., Smirnova, N. S., Rutkevich, P. N., & Vladimirsky, M. A. (2018). Evaluation of the efficiency of lytic mycobacteriophage D29 on the model of M. tuberculosis-infected macrophage RAW 264 cell line. *Bulletin of Experimental Biology and Medicine, 164*(3), 344-346.

Leuenberger, H. (2002). Spray freeze-drying - the process of choice for low water soluble drugs? *Journal of Nanoparticle Research, 4*, 111-119.

Leuenberger, H., Plitzko, M., & Puchkov, M. (2006). Spray Freeze Drying in a Fluidized Bed at Normal and Low Pressure. *Drying Technology, 24*, 711-719.

Leung, S. S., Parumasivam, T., Gao , F. G., Carrigy, N. B., Vehring, R., Finlay, W. H., . . . Chan, H.-K. (2016). Production of Inhalation Phage Powders Using Spray Freeze Drying and Spray Drying Techniques for Treatment of Respiratory Infections. *Pharmaceutical Research, 33*, 1486-1496.

Leung, S. Y., Parumasivam, T., Gao, F. G., Carter, E. A., Carrigy, N. B., Vehring, R., . . . Chan, H.-K. (2017). Effects of Storage Conditions on the Stability of Spray Dried, Inhalable Bacteriophage Powders. *International Journal of Pharmaceutics, 521*, 141-149.

Liu, K.-y., Yang, W.-h., Dong, X.-k., Cong, L.-m., Li, N., Li, Y., . . . Li, J.-s. (2016). Inhalation study of mycobacteriophage D29 aerosol for mice by endotracheal route and nose-only exposure. *Journal of Aerosol Medicine and Pulmonary Drug Delivery, 29*(5), 393-405.

Loc-Carrillo, C., & Abedon, S. T. (2011). Pros and Cons of Phage Therapy. *Bacteriophage, 1*(2), 111-114.

Lu, X., & Pikal, M. J. (2004). Freeze-Drying of Mannitol-Trehalose-Sodium Chloride-Based Formulations: The Impact of Annealing on Dry Layer Resistance to Mass Transfer and Cake Structure. *Pharmaceutical Development and Technology, 9*(1), 85-95.

Malecki, G. (1967, April 11). *US Patent No. 3,313,032.*

Malecki, G. (1970). Atmospheric Fluidized Bed Freeze Drying. *Food Technology, 24*, 93-95.

Manning, M. C., Chou, D. K., Murphy, B. M., Payne, R. W., & Katayama, D. S. (2010). Stability of protein pharmaceuticals: an update. *Pharmaceutical Research, 27*(4), 544-575.

Matinkhoo, S., Lynch, K. H., Dennis, J. J., Finlay, W. H., & Vehring, R. (2011). Spray-dried respirable powders containing bacteriophages for the treatment of pulmonary infections. *Journal of Pharmaceutical Sciences, 100*(12), 5197-5205.

Mensink, M. A., Frijlink, H. W., Hinrichs, W. L., & van der Voort Maarschalk, K. (2017). How sugars protect proteins in the solid state and during drying (review): Mechanisms of stabilization in relation to stress conditions. *European Journal of Pharmaceutics and Biopharmaceutics, 114*, 288-295.

Meryman, H. T. (1959). Sublimation Freeze-Drying without Vacuum. *Science, 130*, 628-629.

Morgan, C. A., Herman, N., White, P. A., & Vesey, G. (2006). Preservation of mico-organisms by drying; A review. *Journal of Microbiological Methods, 66*, 183-193.

Mumenthaler, M., & Leuenberger, H. (1991). Atmospheric spray-freeze drying: a suitable alternative in freeze-drying technology. *International Journal of Pharmaceutics, 72*, 97-110.

Papp-Wallace, K. M., Ednimiani, A., Taracila, M. A., & Bonomo, R. A. (2011). Carbapenems: Past, Present, and Future. *Antimicrobial Agents and Chemotherapy, 55*(11), 4943-4960.

Puapermpoonsiri, U., Ford, S., & van der Walle, C. (2010). Stabilization of bacteriophage during freeze drying. *Interational Journal of Pharmaceutics, 389*, 168-175.

Pyne, A., Surana, R., & Suryanarayanan, R. (2002). Crystallization of Mannitol below Tg' during Freeze-Drying in Binary and Ternary Aqueous Systems. *Pharmaceutical Research, 19*(6), 901-908.

Sadikoglu, H., Ozdemir, M., & Seker, M. (2006). Freeze-drying of pharmaceutical products: research and development needs. *Drying Technology, 24*, 849-861.

Shoyele, S. A., & Cawthorne, S. (2006). Particle engineering techniques for inhaled biopharmaceuticals. *Advance Drug Delivery Reviews, 58*, 1009-1029.

Su, W., Jia, N., Li, H., Hao, H., & Li, C. (2017). Polymorphism of D-mannitol: Crystal structure and the crystal growth mechanism. *Chinese Journal of Chemical Engineering, 25*, 358-362.

Tang, X., & Pikal, M. J. (2004). Design of freeze-drying processes for pharmaceuticals: practical advice. *Phamraceutical Research, 21*(2), 191-200.

Teppler, H., Gesser, R. M., Friedland, I. R., Woods, G. L., Meibohm, A., Herman, G., . . . Isaacs, R. (2004). Safety and tolerability of ertapenem. *Journal of Antimicrobial Chemotherapy, 53*(2), 75-81.

Tice, A. D. (2004). Ertapenem: a new opportunity for outpatient parenteral antimicrobial therapy. *Journal of Antimicrobial Chemotherapy, 53*(2), ii83-ii86.

Trelea, I. C., Passot, S., Fonseca, F., & Marin, M. (2007). An interactive tool for the optimization of freeze-drying cycles based on quality criteria. *Drying Technology, 25*(5), 741-751.

Udwadia, Z. F. (2016). Totally drug resistant-tuberculosis in India: The bad just got worse. *Journal of Association of Chest Physicians, 4*(2), 41-42.

Vandenheuvel, D., Singh, A., Vandersteegen, K., Klumpp, J., Lavigne, R., & Van den Mooter, G. (2013). Feasibility of spray drying bacteriophages into respirable powders to combat pulmonary bacterial infections. *European Journal of Pharmaceutics and Biopharmaceutics, 84*, 578-582.

Wang, H., Barona, D., Oladepo, S., Williams, L., Hoe, S., Lechuga-Ballesteros, D., & Vehring, R. (2017). Macro-Raman spectroscopy for bulk composition and homogeneity analysis of multi-component pharmaceutical powders. *Journal of Pharmacetuical and Biomedical Analysis, 141*, 180-191.

Wang, H., Boraey, M. A., Williams, L., Lechuga-Ballesteros, D., & Vehring, R. (2014). Low-Frequency Shift Dispersive Raman Spectroscopy for the Analysis of Respriable Dosage Forms. *International Journal of Pharmaceutics, 469*, 197-205.

Wang, W. (2000). Lyophilization and development of solid protein pharmaceuticals. *International Journal of Pharmaceutics, 203*, 1-60.

Wang, Z. L., Finlay, W. H., Peppler, M. S., & Sweeney, L. G. (2006). Powder Formation by Atmospheric Spray-Freeze Drying. *Powder Technology, 170*, 45-52.

Waterman, K. C., Adami, R. C., Alsante, K. M., Antipas, A. S., Arenson, D. R., Carrier, R., . . . Wang, H. (2002). Hydrolysis in pharmaceutical formulations. *Pharmaceutical Development and Technology, 7*(2), 113-146.

Webb, S. D., Golledge, S. L., Cleland, J. L., Carpenter, J. F., & Randolph, T. W. (2002). Surrface adsorption of reombinant human interferon-γ in lyophilized and spray-lyophilized formulations. *Journal of Pharmaceutical Sciences, 91*, 1474-1487.

World Health organization. (2018, February 15). Retrieved August 3, 2018, from http://www.who.int/en/news-room/fact-sheets/detail/antimicrobial-resistance

World Health organization. (2018, February 16). Retrieved August 3, 2018, from http://www.who.int/news-room/fact-sheets/detail/tuberculosis

Yoshii, H., Buche, F., Takeuchi, N., Terrol, C., Ohgawara, M., & Furuta, T. (2008). Effects of protein retention of ADF enzyme activity encapsulated in trehlaose matrices by spray drying. *Journla of Food Engineering, 87*, 34-39.

Yu, Z., Johnston, K. P., & Williams III, R. O. (2006). Spray freezing into liqudi versus spray-freeze drying: Influence of atomization on protein aggregation on biological activity. *European Journal of Pharmaceutical Sciences, 27*, 9-18.

Zhang, Y., Peng, X., Zhang, H., Watts, A. B., & Ghosh, D. (2018). Manufacturing and ambient stability of shelf freeze dried bacteriophage powder formulations. *International Journal of Pharmaceutics, 542*, 1-7.